

**PEPTIDE-BASED BIOINSPIRED
FUNCTIONAL MATERIALS**

A THESIS SUBMITTED TO
THE GRADUATE SCHOOL OF ENGINEERING AND SCIENCE
OF BILKENT UNIVERSITY
IN PARTIAL FULFILLMENT OF THE REQUIREMENTS FOR
THE DEGREE OF
MASTER OF SCIENCE
IN
MATERIALS SCIENCE AND NANOTECHNOLOGY

By

OYA ILKE SENTURK

December 2016

PEPTIDE-BASED BIOINSPIRED FUNCTIONAL MATERIALS

By Oya Ilke Senturk

December 2016

We certify that we have read this thesis and that in our opinion it is fully adequate, in scope and in quality, as a thesis for the degree of Master of Science.

Ayşe Begüm Tekinay (Advisor)

Mustafa Özgür Güler (Co-advisor)

Salih Özçubukçu

Hasan Tarık Baytekin

Approved for the Graduate School of Engineering and Science

Ezhan Karışan
Director of the Graduate School

ABSTRACT

PEPTIDE-BASED BIOINSPIRED FUNCTIONAL MATERIALS

Oya Ilke Senturk

MSc in Materials Science and Nanotechnology

Advisor: Ayşe Begüm Tekinay

Co-advisor: Mustafa Özgür Güler

December, 2016

Ability of nature to build complex systems via step-by-step addition of small building blocks with distinctive qualities and multi-functionalities has garnered massive attention which gave a rise to biomimetic or biologically inspired synthesis concept. Biomimetic synthesis mimics nature's approach and design principles offering various combinations of new concepts and designs to adapt them in synthetic materials or processes.[1] Up to date, many efforts have been made to mimic nature's approach for the development and fabrication of more effective synthetic systems and structures to compensate drawbacks and overcome reported challenges in existing models.[2]

In the first part of this thesis, development of a bioinspired, heterogeneous and recyclable Cu-complex catalyst for [3+2] Huisgen cycloaddition reaction, also known as click reaction, is described. A copper binding peptide sequence, human tripeptide Gly-His-Lys (GHK), is utilized for such purpose.[3] GHK sequence is linked with an alkyl tail comprising 6, GHK-6-abx, or 11, GHK-11-adx, carbons to the polystyrene ring amide resin where it is used as a solid support and complexed

with Cu(II). The catalyst provides better catalytic activities in aqueous solvent rather than organic solvents which is a desirable property for green chemistry point of view. Accordingly, an enzyme-like catalyst is described where alkyl tail offers hydrophobic regions for organic reagents to be immobilized closer to the Cu(II), catalytic site of the molecule, and increases reaction yields. 80% yield can be obtained from GHK-11-*adx*-Cu complex catalyst in water using Cu(II) loadings as low as 0.5 mol% and catalytic activity can be retained up to three cycles of reactions.

In the second study of this thesis, we developed a versatile system to induce self-assembly of peptide amphiphiles by using light which is a readily available and cheap reagent allowing precise stimulation and providing quick response. For this purpose, a photo-labile calcium chelator, Nitr-T, which releases free Ca²⁺ ions upon irradiation is mixed with a negatively charged E₂-PA. E₂-PA, a negatively charged PA molecule, self-assembles to form a hydrogel in the presence of free Ca²⁺ ions provided by the NitrT-Ca²⁺ complex, and goes back to its solution state when free Ca²⁺ ions are removed from the medium by the addition of EDTA solution. Consequently, swelling characteristics and mechanical properties of any negatively charged Peptide-Amphiphile (PA) can be controlled by using light as stimuli by simply mixing PA solution with NitrT-Ca²⁺ complex without any further modification or covalent modification in the molecule's structure.

In overall, peptide-based, bioinspired functional materials for various applications like catalysts and tissue engineering was reported in the scope of this thesis. Peptides and peptide-amphiphiles present a very useful member in number of biomimetic applications as they are indispensable part of many biological processes capable of performing very complicated tasks.

Keywords: heterogeneous catalysts, bioinspired materials, light-triggered self-assembly, tissue engineering

ÖZET

PEPTİT BAZLI BİYOESİNLENİLMİŞ FONKSİYONEL MALZEMELER

Oya İlke Şentürk

Malzeme Bilimi ve Nanoteknoloji, Yüksek Lisans

Tez Danışmanı: Ayşe Begüm Tekinay

Tez Eşdanışmanı: Mustafa Özgür Güler

Aralık, 2016

Doğanın, küçük yapı taşlarının adım adım eklenmesiyle, karmaşık görevleri yerine getirebilecek özgün niteliklere ve çeşitli işlevlere sahip olan karmaşık sistemleri inşa etme kabiliyeti, büyük ilgi görmektedir ve biyomimetik veya biyolojik olarak esinlenmiş sentez konseptinin çıkmasına neden olmuştur.[1] Biyomimetik sentez, karmaşık görevleri yerine getirmekten ve materyal bilimlerindeki mevcut sorunları aşmaktan uzak olan sentetik materyal veya proseslere uyarlamak için, yeni kavram ve tasarımların çeşitli kombinasyonlarını sunan doğanın yaklaşımını ve tasarım ilkelerini taklit eder. Varolan modellerdeki dezavantajları aşmak ve bildirilen zorlukların üstesinden gelmek amacıyla daha etkili sentetik sistemlerin ve yapıların geliştirilmesi ve üretilmesi için doğanın yaklaşımını taklit istenmektedir. [2]

Bu tezin ilk bölümünde, click reaksiyonu olarak da bilinen [3 + 2] Huisgen siklo katkılama reaksiyonu için biyomimetik, heterojen ve geri dönüşümlü Cu-kompleks katalizörü geliştirilmiştir. Bu amaçla bir bakır bağlayıcı peptit sekansı olan, insan tripeptidi, Gly-His-Lys (GHK) kullanılmıştır.[3] GHK sekansı, katı-destek olarak ve

Cu(II) ile kompleks hale getirilmiş polistiren Ring amid resinine 6, GHK-6-abx, veya 11, GHK-11-adx, karbon içeren bir alkil sekansı ile bağlanmıştır. Katalizör, yeşil kimya açısından arzu edilen bir şekilde, organik çözücüler yerine sulu çözücüde daha iyi katalitik etkinlik sağlamıştır. Buna göre, alkil sekans, organik reaktifler için, molekülün Cu(II), katalitik bölgesine daha yakın bir yerde hareketsiz kılınacak hidrofobik bölgeler sunar ve reaksiyon verimlerini arttıran enzim benzeri bir katalizör tarif edilmektedir. 0.5 mol % kadar düşük Cu (II) miktarlar kullanarak suda GHK-11-adx-Cu kompleks katalizöründen % 80 verim elde edilebilir ve katalitik aktivite üç döngüye kadar tutulabilmiştir.

Bu tezin ikinci çalışmasında, hassas kontrol ve hızlı tepki sağlayan, kolaylıkla temin edilebilen ve ucuz bir reaktif olan ışık kullanılarak peptit amfifillerin öztoplanmasına neden olacak çok yönlü bir sistem geliştirilmiştir. Bu amaçla, ışınlama üzerine Ca^{2+} iyonlarını serbest bırakan foto-labil kalsiyum şelatör maddesi Nitr-T, negatif yüklü E_2 -PA ile karıştırılmıştır. Negatif yüklü bir PA molekülü olan E_2 -PA, NitrT- Ca^{2+} kompleksi tarafından sağlanan serbest Ca^{2+} iyonlarının varlığında bir hidrojel oluşturacak şekilde öztoplanır ve EDTA çözeltisinin ilavesi ile serbest Ca^{2+} iyonları ortamdan uzaklaştırıldığında çözelti durumuna döner. Sonuç olarak, herhangi bir negatif yüklü Peptit-Amfifilin (PA) şişme özellikleri ve mekanik özellikleri NitrT- Ca^{2+} kompleksiyle basitçe karıştırarak molekül yapısında herhangi bir başka modifikasyon veya kovalent modifikasyon yapmaksızın ve uyarı olarak ışığı kullanarak kontrol edilebilir.

Genel olarak, bu tez kapsamında katalizörler ve doku mühendisliği gibi çeşitli uygulamalarda kullanılacak peptit-amfifil bazlı, biyoesinlenilmiş fonksiyonel malzemeler anlatılmaktadır. Peptitler ve peptit-amfifiller, çok karmaşık görevleri

yerine getirebilmeleri sebebiyle çeşitli biyomimetik uygulamalar için yararlı bir malzeme sunmaktadır.

Anahtar kelimeler: Heterojen katalizörler, biyoesinlenilmiş malzemeler, ışıktan tetiklenen öztoplanım, doku mühendisliği

ACKNOWLEDGEMENT

I would like to thank Prof. Mustafa Özgür Güler and Prof. Ayşe Begüm Tekinay for their support throughout my graduate studies. They were always there for me anytime I needed help and guidance and they steered me in the right direction.

I would like to thank Dr. M. Aref Khalily for his contribution and guidance to my studies and also his companionship and support throughout my masters. I would also like to thank our former lab members Dr. Göksu Çınar, Dr. Melis Şardan Ekiz, Egemen Deniz Eren for their help and their valuable comments throughout my studies.

I would like to express my special thanks to F. Begüm Dikeçoğlu for her support and friendship during stressfull and challenging times we went through.

I would like to acknowledge my lab mates Canelif Yılmaz, İbrahim Çelik, Seren Hamsici, Gökhan Günay, Çağla Eren, Alper Devrim Özkan, Ahmet Emin Topal, Dr. Ruslan Garifullah, Zeynep Orhan, Dr. Özlem Erol, Dr. Gülcihan Gülseren, Mustafa Beter, İdil Uyan, Nuray Gündüz, Gülistan Tansık and Fatih Yergöz for providing a peaceful working environment and their support.

Finally, I must express my very profound gratitude to my dearest friend Ezgi Aydın, for her love, friendship and encouragement, to my dear friend Fırat Rozkan Kılıç for his assistance in forming this thesis, to my parents for their unconditional love and support they gave for my whole life and to my brother, who always be there for me for his valuable guidance and inspiration and also to my beloved not so little cat, kedibey.

CONTENTS

ABSTRACT	iii
ÖZET.....	vi
ACKNOWLEDGEMENT	ix
CONTENTS	x
List of Figures.....	xiii
List of Tables	xvi
Abbreviations.....	xvii
Chapter 1	1
1.1. Fabrication of Bioinspired Materials: Top-down vs. Bottom-up Approach	2
1.2. Peptide-Based Materials	3
CHAPTER 2.....	6
A BIOINSPIRED RECYCLABLE GHK- PEPTIDE CU-COMPLEX CATALYST FOR MODEL [3+2] HUISGEN CYCLOADDITION REACION .	6
2.1. INTRODUCTION	7
2.1.1. [3+2] Huisgen Cycloaddition Reaction	9
2.2. EXPERIMENTAL SECTION	13
2.2.1. Materials.....	13
2.2.2. Synthesis of GHK Peptides and Characterizations.....	13
2.2.3. Copper Complex Formation.....	15
2.2.4. UV-VIS Measurements	16

2.2.5.	Inductively Coupled Plasma – Mass Spectrometer	16
2.2.6.	X-Ray Photoelectron Spectra (XPS) Studies	16
2.2.7.	Scanning Electron Microscopy	17
2.2.8.	General Procedure for Click Reaction.....	17
2.2.9.	Gas Chromatography- Mass Spectroscopy (GC-MS)	17
2.2.10.	Nuclear Magnetic Resonance (NMR)	17
2.2.11.	Recycling of Catalysts.....	18
2.3.	RESULTS AND DISCUSSION	18
2.4.	CONCLUSION	36
CHAPTER 3.....		37
PHOTORESPONSIVE SELF-ASSEMBLY OF PEPTIDE AMPHIPHILES ...		37
3.1.	INTRODUCTION	38
3.1.1	Cages	40
3.2.	EXPERIMENTAL SECTION	41
3.2.1.	Materials.....	41
3.2.2.	Peptide-Amphiphile Synthesis, Characterization and Purification	42
3.2.3.	Nuclear Magnetic Resonance (NMR)	44
3.2.4.	High Performance Liquid Chromatography (HPLC)	44
3.2.5.	Ca ²⁺ -Nitr-T Complex Formation.....	44
3.2.6.	Preparations of Hydrogels.....	44
3.2.7.	Rheological Analyses	45
3.3.	RESULTS AND DISCUSSION	45
3.4.	CONCLUSION	54

CHAPTER 4.....	55
CONCLUSION & FUTURE PROSPECTS.....	55
Bibliography	59

List of Figures

Figure 1.1 Schematic representation of top-down and bottom-up approaches for micro- and nano-fabrication. Strategies utilized in top-down approach from 1 to 4; ink-jet printing, capillary assembly, photo-lithography and nanoimprinting lithography, respectively Strategies utilized in bottom-up approach from 1 to 4; host-guest chemistry, covalent immobilization, layer-by-layer deposition and self-assembly, respectively. (Adapted with permission from ref.[30])	3
Figure 2.1.1 Schematic representation of [3+2] Huisgen cycloaddition reaction.....	9
Figure 2.1.2 A possible reaction mechanism proposed for [3+2] Huisgen cycloaddition reaction (Adapte with permission from Ref.[130] Copyright (2016) American Chemical Society.....	11
Figure 2.3.1 Schematic presentation of GHK-Cu ²⁺ catalyzed [3+2] Huisgen cycloaddition reaction.....	19
Figure 2.3.2 Schematic representation of preperation of GHK-abx-6-Cu complex catalyst and photographic image of the complex	20
Figure 2.3.2 A) Chemical representation og GHK-6-abx PA, B) MS-ESI data of GHK-6-abx PA [M] _{calculated} =453.54, [M+Na ⁺] _{calculated} =475.27, [M] _{observed} =453.29, [M+Na ⁺] _{observed} =475.27, C) Chemical representation of GHK-11-adx PA, D) MS-ESI data of GHK-11-adx PA [M] _{calculated} =523.68, [M+Na] _{calculated} =545.34, [M] _{observed} =523.36, [M+Na ⁺] _{observed} =545.41	21
Figure 2.3.3 A) SEM images of PS-GHK-6-abx-Cu(II) complex, B) EDX Studies conforming the presence of Cu(II) on beads	23

Figure 2.3.4 Schematic representation of click reaction between benzyl azide and phenyl acetylene	24
Figure 2.3.5 XPS Survey data of GHK-6- <i>adx</i> -Cu a) before usage, c) after usage, Cu survey data b) before usage, d) after usage (smoothing at polynomial 8)	25
Figure 2.3.6 XPS Survey data of GHK-11- <i>abx</i> -Cu a) before usage, c) after usage, Cu survey data b) before usage, d) after usage (smoothing at polynomial 8)	26
Figure 2.3.7 UV-VIS spectra of GHK-6-Cu catalyst in DMF A) before use, B) after use. An absorption peak around 650 nm which is assigned to Cu ²⁺ -imidazole complex.....	28
Figure 2.3.8 Recyclability of GKH-11- <i>adx</i> -Cu complex to afford 1,2,3 triazole product, at 40 °C for 40 h	31
Figure 2.3.9 GC-MS analysis of 1-benzyl-4-phenyl-1H-1,2,3 A) Chromatogram of reaction mixture comprising 1:1 MeOH-H ₂ O, at 40 °C, after 40 h, B) Mass Spectrometry data of the product MS (C ₁₅ H ₁₃ N ₃) _{calculated} =239.29, MS (C ₁₅ H ₁₃ N ₃) _{observed} =235.1	32
Figure 2.3.10 A. ¹ H-NMR of 1-benzyl-4-phenyl-1H-1,2,3-triazole in CDCl ₃	34
Figure 2.3.10 B. ¹³ C-NMR of 1-benzyl-4-phenyl-1H-1,2,3-triazole in CDCl ₃	35
Figure 3.3.1 A) Molecular structure of Nitr-T molecule, before and after photolysis, Nitr-T-Ca ²⁺ complex. Adapted with permission from Ref.[171] Copyright (2016) American Chemical Society B) Chemical representation of Lauryl-VVAGEE-Am PA (E ₂ -PA) C) Schematic representation of photo-triggered gelation of E ₂ -PA with Nitr-T.	46
Figure 3.3.2 Liquid Chromatography-Mass Spectrometry (LC-MS) analyses of E ₂ -PA.....	47
Figure 3.3.3 Rheological analysis of 2 wt % E ₂ -PA-Ca ²⁺ gel.....	48

Figure 3.3.4 ¹ H-NMR Spectrum of Nitr-T tetraethyl ester.....	50
Figure 3.3.5 Rheological analyses of only 2.0 wt % E ₂ -PA, E ₂ -PA w/Nitr-T and E ₂ -PA w/Nitr-T after 30 minutes of UV treatment B) Modulus values with error bars collected from the samples at t=20 min, N=3.....	51

List of Tables

Table 2.3.1 Reaction yields of click reaction in different solvents, GHK-6-abx-Cu complex was used as catalyst, reaction proced at 50 °C for 40.....	24
Table 2.3.1 Reaction yields of click-reactions when GHK-6-abx-Cu complex and GHK-11-adx-Cu complex was used as the catalyst in different solvent system.....	29
Table 2.3.2 Reaction yields of click-reactions when GHK-6-abx-Cu complex and GHK-11-adx-Cu complex was used as the catalyts in different solvent systems, at 40 °C, 40 h.....	31

Abbreviations

DCM	Dichloromethane
DIEA	<i>N,N</i> -diisopropylethylamine
DMF	<i>N,N</i> -dimethylformamide
EtOAc	Ethyl acetate
Fmoc	9-Fluorenylmethoxycarbonyl
HPLC	High performance liquid chromatography
HBTU	<i>N,N,N',N'</i> -Tetramethyl- <i>O</i> -(1 <i>H</i> -benzotriazole-1-yl) uronium hexafluorophosphate
LC-MS	Liquid chromatography-mass spectroscopy
NMR	Nuclear magnetic resonance
PA	Peptide amphiphile
QTOF	Quadrupole time of flight
RT	Room temperature
SEM	Scanning electron microscopy
SPPS	Solid phase peptide synthesis
TFA	Trifluoroacetic acid
XPS	X-ray photoelectron spectroscopy
CuAAC	Copper Catalyzed Cycloaddition Reaction
abx	6-Aminohexanoic acid
adx	11-Aminoundecanoic acid

Chapter 1

1. Introduction

In early stages of civilization, humans were aided by natural materials such as rocks, wood and bone. However, as technology advanced, these natural materials were replaced by synthetic materials that presented better performances. Traditionally, chemists are proficient at producing new synthetic materials and altering their micro- and macroscale organization through molecular synthesis methods; however, doing so requires expensive, time-consuming and highly specialized protocols and equipment. Nature, on the other hand, has a fascinating ability to form complex architectures that simultaneously exhibit multiple functionalities and perform complicated tasks that are far from being accomplished by synthetic systems.[1] As such, biology possesses an infinite number of combinations of new approaches which can revolutionize every aspect of materials science in terms of fabrication, design, and functionality. For this reason, biological materials existing in nature have been studied extensively for decades and have facilitated the emergence of bioinspired design strategies, which adapt the design principles and approaches used by nature for the development of synthetic systems.[2]

Biologically inspired or biomimetic synthesis is a non-conventional and interdisciplinary approach that is at the interphase of material science, biology, physics and chemistry.[4] The integration of these fields has allowed rapid progress in material design principles, and many biomimetic material concepts, such as light-harvesting, photosynthesis-mimicking photonic materials, advanced photonic structures that mimic butterfly wings, structural nacre-like composites for flaw

tolerance, gecko-inspired reversible adhesives and mussel-inspired, water-tolerant adhesives are currently under development.[5–13] In addition, the use of bioinspired materials is also under investigation for biological applications such as regenerative medicine, drug delivery and tissue engineering, energy conversion and storage, and the design of enzyme-mimetic catalysts.[14–21]

1.1. Fabrication of Bioinspired Materials: Top-down vs. Bottom-up Approach

Two main approaches exist for fabricating functional materials: top-down and bottom-up approaches. In the top-down approach, nanofabrication tools designed for cutting, milling and etching are controlled externally to form structures in desired shapes and properties from bulk materials.[22] Micro-cutting techniques such as lithographic techniques and inkjet printing are commonly used for this approach.[23], [24] Although a range of top-down approaches have been utilized to successfully produce bioinspired materials, the use of bottom-up approaches is more favored for fabricating bioinspired materials, as the latter is used by natural organisms to produce extremely complex systems like proteins.[25–27] In the bottom-up approach, complex systems are assembled through the step-by-step addition of small building blocks, *i.e.* molecules or atoms, into a precisely designed structure.[26] Until now, considerable efforts have been made in order to mimic nature's bottom-up approach covering concepts like molecular recognition and self-assembly.[28]

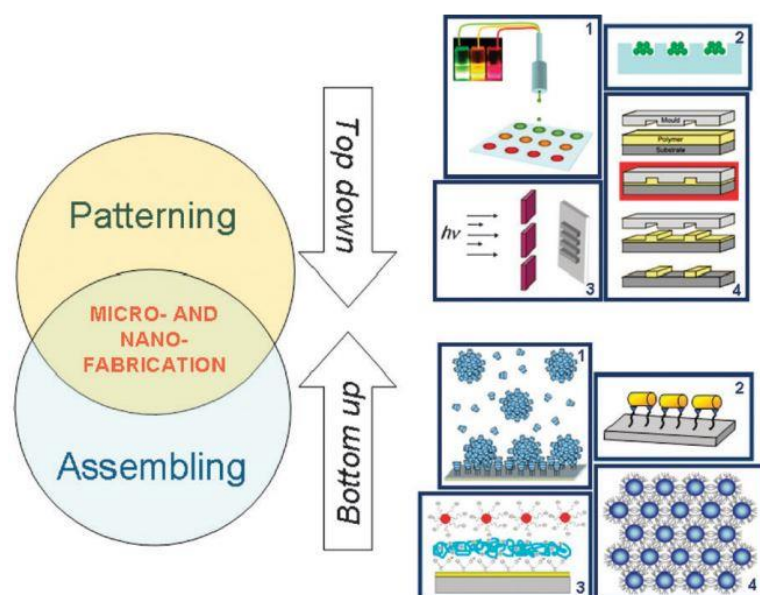


Figure 1.1 Schematic representation of top-down and bottom-up approaches for micro- and nano-fabrication. Strategies utilized in top-down approach from 1 to 4; ink-jet printing, capillary assembly, photo-lithography and nanoimprinting lithography, respectively Strategies utilized in bottom-up approach from 1 to 4; host-guest chemistry, covalent immobilization, layer-by-layer deposition and self-assembly, respectively. (Adapted with permission from ref.[29])

1.2. Peptide-Based Materials

Peptides are biologically occurring molecules consisting of chains of amino acids, which are organic compounds containing an amine group (NH_2), a carboxyl group (COOH), and a side chain (R group) linked by amide (peptide) bonds.[30] Side chains (R) are mainly responsible for determining the chemical and physical properties of amino-acids and, consequently, the peptides they constitute.[30] In nature, protein domains and peptides play a very important role in many biological events through their complex and variable functions. For example, elastin modulates cell behavior by modulating mechanical properties of extracellular matrix (ECM), RGD provides discrete biological cues for cell adhesion, S-layer proteins protect

bacterial cells by assembling into well-organized structures on cell membranes, and enzymes catalyze reactions beyond the scope of current synthetic chemistry with very high efficiencies and selectivities at millisecond-level time scales and without the formation of unwanted byproducts.[31–34] These functions of peptides and proteins can be borrowed from nature and integrated into synthetic systems to provide them with bio-inspired functions. Consequently, peptides present an important platform to construct novel complex structures where both biological specificity and multifunctionality can be incorporated into organic, inorganic or carbon-based materials; moreover, structure and properties of the materials can be controlled.[35] Therefore, a great variety of peptides, consisting of different amino acid sequences with different lengths, have been recently used for the synthesis or functionalization of materials ranging from nanoparticles for catalysis, assembly, sensing and recognition applications; to polymers for biological and nonbiological applications; and to metal organic frameworks (MOFs) for hydrogen storage and recognition applications. [35–40] For example, a number of recent studies have reported that peptide nanofibers decorated with Pd nanoparticles can serve as efficient catalysts for a broad range of reactions, such as Suzuki coupling reactions and the synthesis of sulfides under aerobic and mild conditions.[38, 41, 42]

Peptides themselves were also found to be very useful in a number of applications, and are commonly used as enzyme mimetic catalysts, bio-adhesives and scaffolds for materials synthesis, drug delivery, tissue scaffolding and bio-mineralization applications.[14, 16, 43–46] For instance, enzyme mimetic peptides can be used to effectively catalyze reactions that do not occur readily under ambient conditions, such as nanoparticle synthesis, or they can enable reactions that require an organic

environment to proceed under aerobic conditions.[44, 47–49] Another major application of peptides lies in the development of ECM-mimetic peptide hydrogels, which can be decorated with bio-active peptide sequences providing specific biological cues and mechanical properties for tissue engineering applications.[50–52]

CHAPTER 2

A BIOINSPIRED RECYCLABLE GHK- PEPTIDE CU- COMPLEX CATALYST FOR MODEL [3+2] HUISGEN CYCLOADDITION REACION

2.1. INTRODUCTION

There are two main sub-categories determining the synthetic efficiency of an organic synthesis, which are atom economy and selectivity.[53, 54] High selectivity results in minimizing the byproducts of a reaction, eliminating the need for their subsequent elimination, while atom economy is an important factor in green chemistry and serves as a metric for measuring the "greenness" of a synthesis.[53–56] Developing synthetic routes, reactions and reagents achieving both selectivity and atom economy is one of the main goals of synthetic chemistry. Emergence of transition metals to catalyze organic reactions in 1960s has changed the course of organic synthesis by addressing both selectivity and atom economy issues and enabling the development of countless synthetic routes.[55, 57, 58] Transition metal-catalyzed reactions are considered as one of the most straightforward, efficient and reliable tools for the development of one-step synthesis methods for complex structures in organic chemistry.[59, 60] Some examples of organic reactions catalyzed by transition metals include Kumada, Negishi, Suzuki-Miyaura, Sonogashira, Stille and Buchwald-Hartwig coupling reactions, Heck reactions, hydrogenation, hydrocarboxylation and hydroesterification reactions, alcohol oxidation reactions, allylic substitution reactions, carbonmonoxide oxidation reactions and the Huisgen 1,3-dipolar cycloaddition reaction which are catalyzed mainly by the transition metals Pd, Ni, Co, Au, Fe or Cu.[38, 61–79] Most of these reactions are carried out by homogeneous catalysts, which are catalysts that are in the same phase as the reactants.[80, 81] Since the catalyst is present in the reaction media as a soluble metal complex, all of its catalytic sites are accessible; therefore, enantio-, chemo- and regio-selectivity of the catalyst can be adjusted.[82] Besides high selectivity,

homogeneous catalysts also offer high reactivity, better yield, high turnover number (TON) and a facile system optimization process through the modification of metals and ligands.[81, 82] Despite these advantages, homogenous catalysts remain in the reaction mixture after the completion of the reaction, thereby imposing additional costs and difficulties associated with their separation from the product by conventional methods such as chromatography, distillation and extraction. Consequently, their application is limited.[57, 81] Metal contamination in particular is a major issue, as it is unacceptable in electronics and causes toxicity in biological applications; the removal of metal catalysts from the products is therefore essential.[83] In addition, the high amounts of waste created by these reactions have raised environmental concerns, as the catalysts cannot be reused and lengthy and expensive procedures are required to remove metals from the products.[81, 84]

Tremendous efforts have been made to overcome these problems and increase reaction efficiency under moderate reaction conditions through reusable and recyclable catalytic substances. Heterogeneous catalysts, which are in a different phase with the reaction mixture and incorporate the metal catalyst on an insoluble support through a covalent or a non-covalent attachment, have therefore emerged as a potential alternative to homogenous catalysts.[85–87] Heterogeneous catalysts offer many advantages over their homogenous counterparts, including but not limited to minimizing the amount of waste produced after the reaction, consumption of supplementary compounds, and lower investment in money, time and energy to separate transition metals from the reaction products, resulting in significant decrease in costs.[82, 86, 88] Additionally, these catalyst offer better selectivity and are often thermally and chemically stable.[57] These catalysts are similar to enzyme catalysis

in terms of recyclability, and they can be easily recovered from the reaction mixture with straightforward methods such as simple filtration, decantation or magnetic recovery to be used over and over again.[57, 79, 89] Previously reported support materials include carbon, ordered or amorphous silicates, zeolites, magnetic-materials, and soluble and insoluble polymers.[77, 78, 89–99]

2.1.1. [3+2] Huisgen Cycloaddition Reaction

In modern pharmaceuticals industry, simple methods enabling the generation of large libraries of compounds are desired and commonly used.[100, 101] Huisgen cycloaddition, an exergonic fusion process, is an example of such a method and unites alkynes and azides to yield five membered hetero-cycles (1,2,3 triazoles), as shown in Figure 2.1.1.[102]

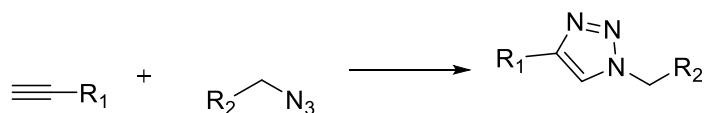


Figure 2.1.1 Schematic representation of [3+2] Huisgen cycloaddition reaction

Due to the wide scope of applicability, high yields, 100% atom economy, high selectivity and simple purification of the reaction, Huisgen cycloadditions have become a very important type of reaction in organic chemistry.[103, 104] However, the original reaction requires high reaction temperatures and displays low regioselectivity, which has limited its application.[103, 105] After the discovery made by Meldal and Sharpless, in which presence of Cu(I) in the reaction mixture as a catalyst dramatically increases reaction rates under mild conditions and results in high regioselectivity towards 1,4 disubstituted regioisomer of the triazole product, Huisgen cycloadditions garnered enormous attention and have become one of the

most robust and useful click reactions.[104, 106], 107] Since then, click version of Huisgen cycloaddition (Copper (I)-catalyzed azide-alkyne cycloaddition, CuAAC) has thus been extensively applied for the material science, chemical and combinational synthesis, polymer and dendrimer synthesis, functionalization of biomolecules, and bioconjugation.[108–118] Additionally, members of the 1,2,3 triazole family possess an important role in pharmaceutical industry owing to their stability, lack of toxicity, and ability to mimic peptide bonds without being sensitive towards hydrolytic cleavage, in addition to their interesting biological properties, such as anti-allergic, anti-HIV activity and anti-bacterial effects.[103, 119–125] Furthermore, some members of the family have enjoyed widespread industrial usage as corrosion inhibitors, photo-stabilizers and dyes.[126–128]

The copper(I) species is essential for CuAAC reactions, the proposed mechanism for which is shown in Figure 2.1.2. Cu(I) has been traditionally produced *in situ* in the reaction mixture from CuSO₄ and sodium ascorbate, which reduces Cu(II) to obtain the monovalent copper species.[106]

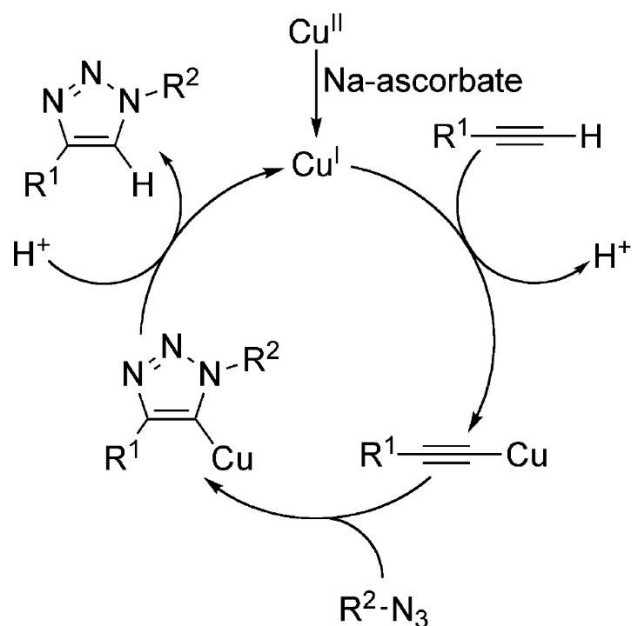


Figure 2.1.2 A possible reaction mechanism proposed for [3+2] Huisgen cycloaddition reaction (Adapte with permission from Ref.[129] Copyright (2016) American Chemical Society

Alternatively, *in situ* oxidation of Cu(0) or the introduction of Cu(I) salts directly to the reaction medium has also been used to catalyze the reaction.[130, 131] Nevertheless, the *in situ* preparation of catalyst from CuSO₄ derivatives is reported to be more preferable, as they are purer than Cu(I) salts, incur lower costs, and result in higher yields and limited byproduct formation.[106] Then again, the conventional and practical “CuSO₄ and sodium ascorbate” catalyst also suffers from several previously mentioned disadvantages associated with homogeneous catalysts, such as difficulties in the disposal of copper from reaction products, low regioselectivity, and being non-recyclable.[92] Moreover, stoichiometric or higher quantities of CuSO₄ are required for CuAAC, which also makes catalyst removal challenging and limits the application of the reaction.[132, 133] Many heterogeneous copper catalysts, in which copper is immobilized on silica, polymer, zeolites, chitosan and charcoal, have been developed to overcome this problem.[78, 84, 88, 90–92, 129, 134, 135]

Recently, a very robust, amphiphilic-polymeric, copper catalyst system with very high efficiency was reported for CuAAC reactions by Yadama *et al.*, who were inspired by the structure of copper metalloenzymes, which are metal-organic hybrids of imidazole-containing peptides and copper ions that promote enzymatic reactions with high efficiencies.[129, 136] As reported in the study, complexation of copper species and imidazole moieties in histidine provides both Lewis acidic-Brønsted basic catalytic sites and a supramolecular tertiary structure, making imidazole-supported copper catalysts very attractive for organic chemistry.[129, 135, 137]

Here we report a bioinspired metal-binding GHK peptide sequence for the straightforward immobilization of Cu ions as a recyclable Click Reaction (CuAAC) catalyst. In this system, the human peptide Gly-(L-His)-(L-Lys) or GHK, which is also known as copper peptide and has an unusual affinity towards Cu^{2+} , was linked with a six- or eleven-carbon alkyl tail to a polystyrene resin, which is used both as a solid support and to facilitate the complexation of copper with the linked GHK peptide.[3] This design is recyclable and can be prepared using a short and facile synthesis pathway compared to other heterogeneous catalysts, which makes it possible to produce the catalyst in gram and kilogram scales. In addition, the copper/peptide system readily functions in environments under ambient conditions due to the inertness and thermal stability provided by the polystyrene support. The resin-immobilized GHK- Cu^{2+} complex successfully catalyses CuAAC up to three cycles in aqueous environment without a significant loss of reaction yields. Organic reagents were immobilized at hydrophobic regions provided by the alkyl linker, which makes them closer to the active sites and increases reaction yields by acting like enzymes.

2.2. EXPERIMENTAL SECTION

2.2.1. Materials

All reactions and syntheses were conducted under atmospheric pressure and at room temperature, unless otherwise noted. All solvents, reagents, acids and bases used were in analytical grade and were purchased from the commercial suppliers Invitrogen, Fisher, Merck, Alfa Aesar, and/or Sigma-Aldrich. Fmoc-11-Amino-undecanoic acid, Fmoc-6-amino-hexanoic acid, benzyl azide, phenyl acetylene, $\text{CuSO}_4 \cdot 5\text{H}_2\text{O}$ and all solvents used in syntheses were in analytical grade and were purchased from Sigma Aldrich. Rink amide MBHA resin (0.78 mmol/g loading), all Fmoc-protected amino acids, diisopropylethylamine (DIEA) and *N,N,N',N'*-tetramethyl-*O*-(1*H*-benzotriazole-1-yl) uronium hexafluorophosphate (HBTU) were purchased from Merck Milipore, Novabiochem. All water used was deionized in a Milli Q purification system.

2.2.2. Synthesis of GHK Peptides and Characterizations

2.2.2.1 GHK-C₆-abx Synthesis

GHK-abx-C₆ PA was synthesized on MBHA ring amide resin at 0.5 mol scale via conventional Fmoc-based solid phase peptide synthesis. Fmoc-6-amino-hexanoic acid, Fmoc-Lys(Mtt)-OH, Fmoc-His(Mmt)-OH and Gly-(Fmoc)-OH were used for the synthesis. Amino acid couplings were done by mixing 2 equivalents of Fmoc-protected amino acid, 1.95 equivalents of HBTU, and 3 equivalents of DIEA in dimethylformamide (DMF) for 1 equivalent of ring amide resin and shaking the mixture for 4 h. After each coupling, to prevent formation of byproducts, uncoupled N-terminal amine was acetylated with 10% acetic anhydride-DMF solution by

shaking the resin for 30 min. Fmoc groups were removed by shaking the reaction vessel with 20% piperidine/dimethylformamide (DMF) solution for 20 min. Following each step, the resin was washed thoroughly three times with dimethylformamide (DMF), then with dichloromethane (DCM) and with dimethylformamide (DMF) again, respectively. After the couplings, to remove 4-methyltrityl (Mtt) and Monomethoxytrityl (Mmt) protecting groups, resin was treated with 5% TFA cleavage cocktail containing TFA: TIS: H₂O: DCM in the ratio of 5: 2.5: 2.5: 90 for 5 min sessions, for 6 times and washed thoroughly with DCM after each treatment. Bright yellow color of the treatment and washing solution indicated the presence of mmt and mtt groups.

2.2.2.2 GHK-C₁₁-adx Synthesis

GHK-abx-C₆ PA was synthesized on MBHA ring amide resin at 0.5 mol scale via Fmoc-based solid phase peptide synthesis. Fmoc-11-amino-undecanoic acid, Fmoc-Lys(Mtt)-OH, Fmoc-His(Mmt)-OH and Gly-(Fmoc)-OH were used for the synthesis. Amino acid couplings were done by mixing 2 equivalents of Fmoc-protected amino acid, 1.95 equivalents of HBTU, and 3 equivalents of DIEA in dimethylformamide (DMF) for 1 equivalent of ring amide resin and shaking the mixture for 4 h. After each coupling, to prevent formation of byproducts, uncoupled N-terminal amine was acetylated with 10% acetic anhydride-DMF solution by shaking the resin for 30 min. Fmoc groups were removed by shaking the reaction vessel with 20% piperidine/dimethylformamide (DMF) solution for 20 min. Following each step, the resin was washed thoroughly three times with dimethylformamide (DMF), then with dichloromethane (DCM) and with dimethylformamide (DMF) again, respectively. After the couplings, to remove 4-methyltrityl (Mtt) and Monomethoxytrityl (Mmt)

protecting groups, resin was treated with 5% TFA cleavage cocktail containing TFA: TIS: H₂O: DCM in the ratio of 5: 2.5: 2.5: 90 for 5 min sessions, for 6 times and washed thoroughly with DCM after each treatment. Bright yellow color of the treatment and washing solution indicated the presence of mmt and mtt groups.

2.2.2.3 Liquid Chromatography-Mass Spectrometry

Agilent Technologies 6530 Accurate-Mass Q-TOF Mass Spectroscopy with electrospray-ionization (ESI) source was used to perform liquid chromatography-mass spectrometry for characterization of peptides. Small portions from resins were taken, washed thoroughly with DCM and then were cleaved from the resin by shaking them with 95% TFA cleavage cocktail which comprises TFA: TIS: H₂O in the ratio of 95: 2.5: 2.5 for 3 h prior to the analysis. Subsequently, resins were washed with DCM and cleaved peptides were collected in DCM. DCM and TFA were removed from peptides by *vacuo*. Resulting peptides was dissolved in water. The concentration of the sample was adjusted as 1 mg/mL. Water and acetonitrile were used as mobile phase for Mass Spectrometry analyses.

2.2.3. Copper Complex Formation

Polystyrene resins bearing GHK peptide was mixed with excess amount of CuSO₄.5H₂O in DMF. Reaction mixture was stirred and heated to 50°C for 12 h and washed thoroughly with DMF, Milli Q water, DMF and DCM, to get rid of unbound CuSO₄.5H₂O, respectively. Washed resin was dried overnight under vacuum. Color of the resulting resins was blue due to the copper complex.

2.2.4. UV-VIS Measurements

Cary Eclipse UV-VIS-NIR Spectrophotometer (Cary 5000) was used for analysis of resin and copper catalyst to observe the bond formation between imidazole group of the peptides and copper. Presence of Cu-imidazole bond after reusing the catalyst was also tested. DMF was used as solvent for the measurements.

2.2.5. Inductively Coupled Plasma – Mass Spectrometer

To determine the amount of copper stabilized on beads inductively coupled plasma-mass spectrometry (ICP-MS, Thermo X Series II) was utilized. In this method, a calibration curve was derived by dissolving and serially diluting a copper-containing plasma emission standard solution (1000 ppm, VWR-BDH Prolabo) in 2% nitric acid to obtain standard copper solutions containing 500, 250, 125, 62.5 ppb and 31.5 ppb of Cu. 5 mg of beads was dissolved in aqua-regia solution. Beads kept in the solution overnight for the complete dissolution of PS beads. Resulting solution then diluted 1:20 with 2% of HNO₃ solution prior to the measurements.

2.2.6. X-Ray Photoelectron Spectra (XPS) Studies

X-ray photoelectron spectra of polystyrene (PS) resin beads bearing peptide-copper complex were recorded by using Thermo K-alpha monochromatic high performance X-ray photoelectron spectrometer. Resin beads were immobilized on carbon tape. The survey analyses were performed at 10 scans. For enhancing Cu signal intensities, the measurements were recorded at 30 scans.

2.2.7. Scanning Electron Microscopy

FEIQuanta 200 FEG environmental scanning electron microscope (SEM) was used to image PS resin beads after formation of complex and EDX was used to determine the presence of copper on PS beads. Resin beads were immobilized on carbon tape and due to the present copper on beads, Au coating was not required for imaging.

2.2.8. General Procedure for Click Reaction

All reactions and manipulations were run under air atmosphere and at either 50°C or 40°C. A mixture of PS resin bearing GHK-6-abx-Cu or GHK-11-adx-Cu complex (10.0 mg, comprises 8.56×10^{-4} mmol, 0.005 eq. Cu^{2+}), phenyl acetylene (15.9×10^{-2} mmol, 1.0 eq.), benzyl azide (15.9×10^{-2} eq), ascorbic acid (4.2×10^{-2} mmol) was prepared in the indicated solvent systems and stirred at 320 rpm for 40 h. The crude product (1-benzyl-4-phenyl-1H-1,2,3-triazole) was extracted by 2 ml of ethyl acetate (3 times) and organic layers were dried over CaCl_2 . Ethyl acetate was removed by vacuum distillation and the triazole product was collected as a white solid.

2.2.9. Gas Chromatography- Mass Spectroscopy (GC-MS)

An aliquot taken from the organic layer of extraction solution, diluted 1:10 by ethyl acetate and then was characterized by and GC-MS analysis. Agilent GCMS-7890A-5975C equipped with a 0.25 mm \times 30 m HP-5MS capillary column was used. Relative amounts of the product were determined via calibration curve.

2.2.10. Nuclear Magnetic Resonance (NMR)

Bruker DPX-400 MHz (400 MHz for ^1H -NMR and 100 ^{13}C MHz) was used for NMR analysis. 3.0 mg triazole product was dissolved in 0.7 mL of CDCl_3 with tetramethyl

silane (TMS) as internal standard. All measurements were done at 25 °C, chemical shifts were given as ppm.

2.2.11. Recycling of Catalysts

After reactions, PS resin beads were simply filtered and collected from the reaction mixture. Washed thoroughly with DMF, DCM, DMF, water and DCM, respectively. Washed resin beads were dried overnight under the vacuum.

2.3. RESULTS AND DISCUSSION

There remains a need for environment-friendly, easily produced recyclable catalytic systems for transition metal catalysts that perform effectively in aqueous environments, enable the facile recovery of the catalyst from the reaction mixture, and consequently prevent the soluble catalyst from contaminating the final product. Immobilization of transition metals on solid supports offers a platform to meet that need. Therefore, we designed a biomimetic click reaction catalyst composed of a metal-binding GHK peptide sequence that is bound to polystyrene resin with a six- or eleven-carbon alkyl spacer via SPPS. Schematic representation of the process is shown in Figure 2.3.1

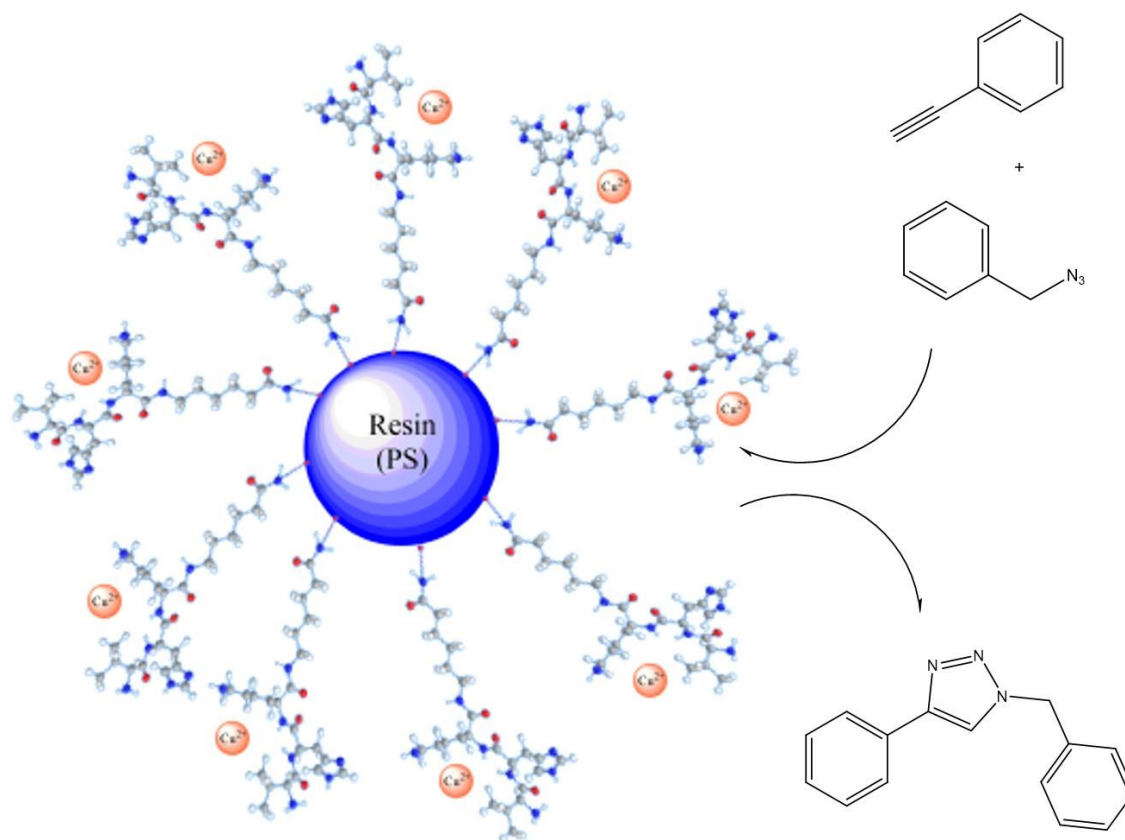


Figure 2.3.1 Schematic presentation of GHK-Cu²⁺ catalyzed [3+2] Huisgen cycloaddition reaction

Molecular structures and MS-ESI data of the GHK-6-abx PA and GHK-11-adx PA are shown in Figure 2.3.3. A small portion of the peptide was cleaved from the PS resin support and used for MS-ESI analyses to confirm the success of the peptide synthesis process. Following the synthesis of peptides on PS resin support, they were complexed with Cu²⁺ by mixing the PS beads with CuSO₄·5H₂O salt in DMF at 50 °C. After 12 h, resin was filtered, washed thoroughly and isolated in quantitative yields. Colorless transparent resins became bluish after the complexation (Figure 2.3.2). After washing out the excess salt, the amount of Cu(II) immobilized on the beads was investigated with ICP-MS analysis. The amount of Cu(II) was determined to be 8.6 x10⁻⁵ mmol/g of resin from calibration curves.

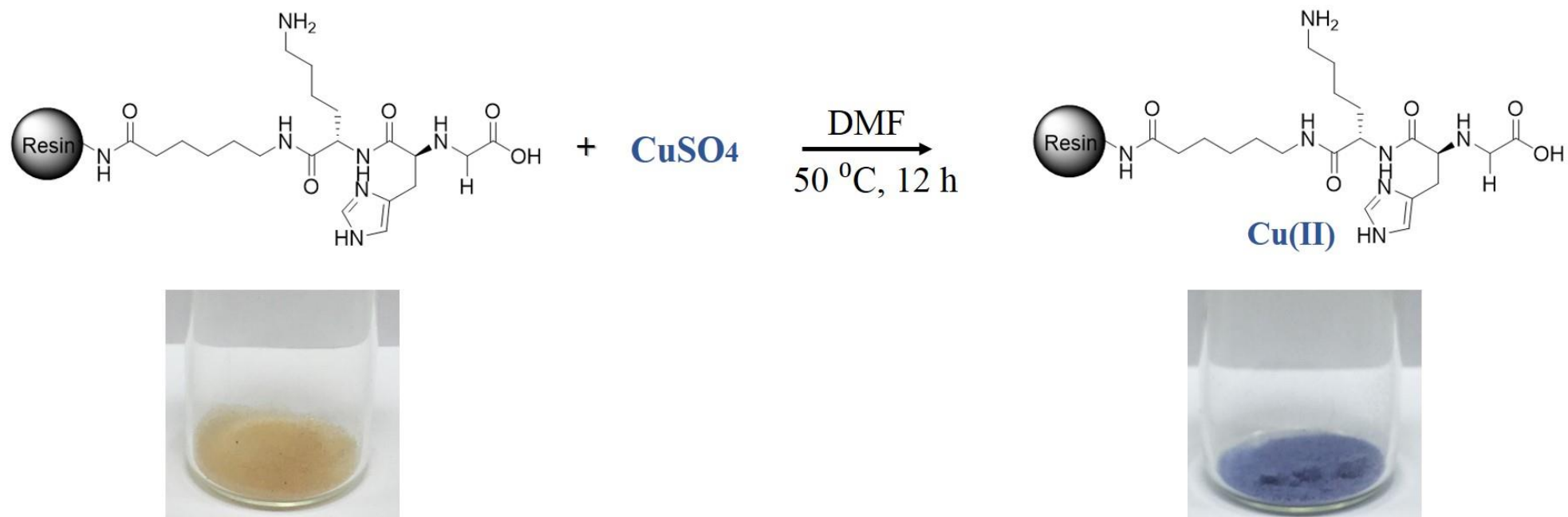


Figure 2.3.2 Schematic representation of preparation of GHK-abx-6-Cu complex catalyst and photographic image of the complex

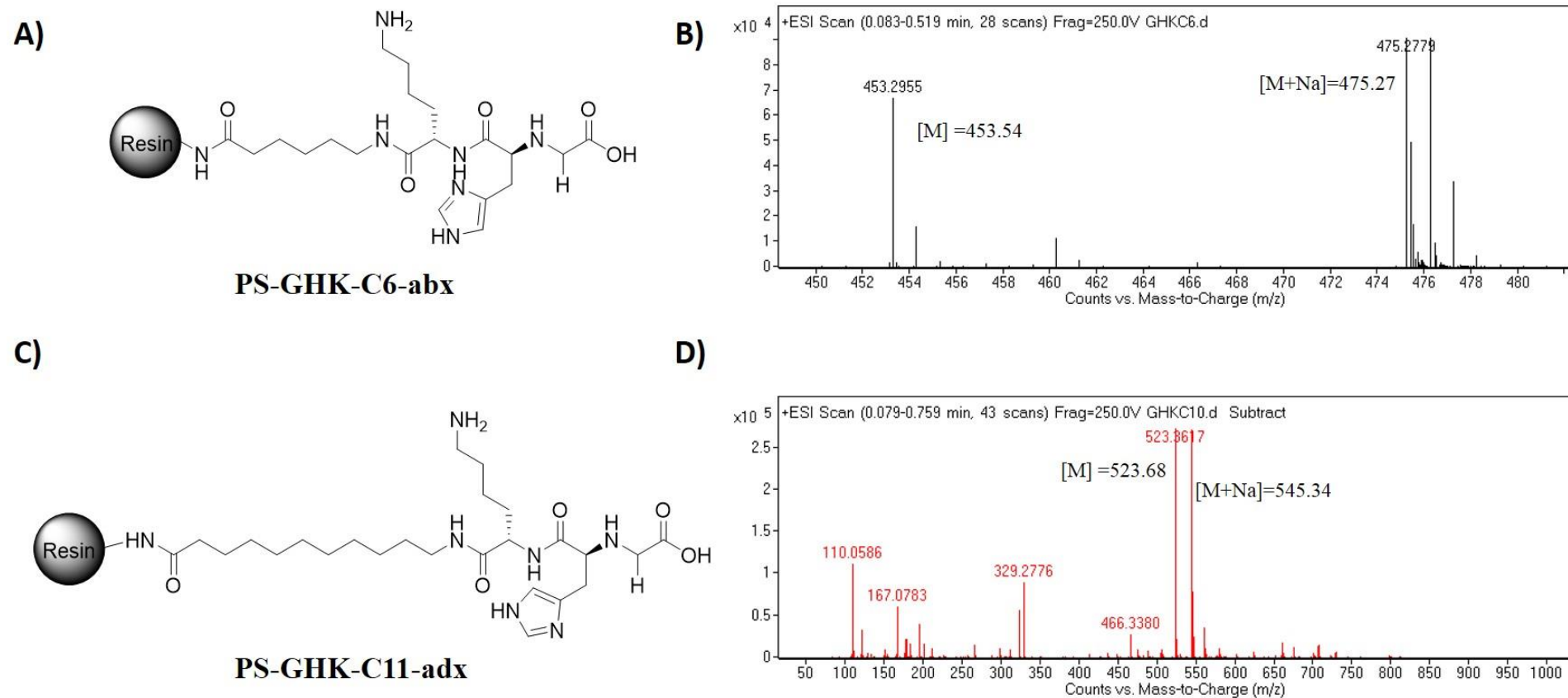


Figure 2.3.2 A) Chemical representation of GHK-6-abx PA, B) MS-ESI data of GHK-6-abx PA $[M]_{\text{calculated}}=453.54$, $[M+Na^+]_{\text{calculated}}=475.27$, $[M]_{\text{observed}}=453.29$, $[M+Na^+]_{\text{observed}}=475.27$, C) Chemical representation of GHK-11-adx PA, D) MS-ESI data of GHK-11-adx PA $[M]_{\text{calculated}}=523.68$, $[M+Na^+]_{\text{calculated}}=545.34$, $[M]_{\text{observed}}=523.36$, $[M+Na^+]_{\text{observed}}=545.41$

Presence of copper on beads was also confirmed with EDX studies, and images of PS beads after complex formation was obtained using scanning electron microscopy (SEM). A sulfur peak attributable to residual sulfate could also be observed in EDX studies, but was at low-intensity compared to the copper peak (Figure 2.3.4 B). Imaging was conducted with carbon tape to preclude intervention by Cu(II) signals coming from copper tape. Au coating was not required for the sample since the presence of copper provided the required conductivity for imaging. As seen on SEM images in Figure 2.3.4.A, no disformation on resin beads was observed after the complexation of copper.

Provided that the Cu(II) is immobilized on the resin, we tested the catalytic activity of the catalyst towards the [3+2] Huisgen cycloaddition reaction (*i.e.* click reaction). Schematic representation of the reaction is shown in Figure 2.3.5. A model click reaction between phenyl acetylene and benzyl azide was monitored using the GHK-6-*adx*-Cu complex as the catalyst in several solvent systems that are commonly used for click reactions. In order to compensate for low catalyst loadings, reaction times were extended to 40 h and the reaction was left to proceed at higher temperatures. During reaction, the bluish color of GHK-6-*adx*-Cu turned green. After 40 h, the product was collected at very high purity by a simple ethyl acetate extraction protocol. As shown in Table 2.3.1, reaction yields were very low for organic solvents like ACN and DMF, while higher yields were obtained as the ratio of water was increased for the *tert*-butanol/H₂O system. Low yields in organic solvents can be attributed to low loadings of catalyst (0.5 mol %) in the system. As water percentage and the hydrophilicity of the environment increases, organic reagents were

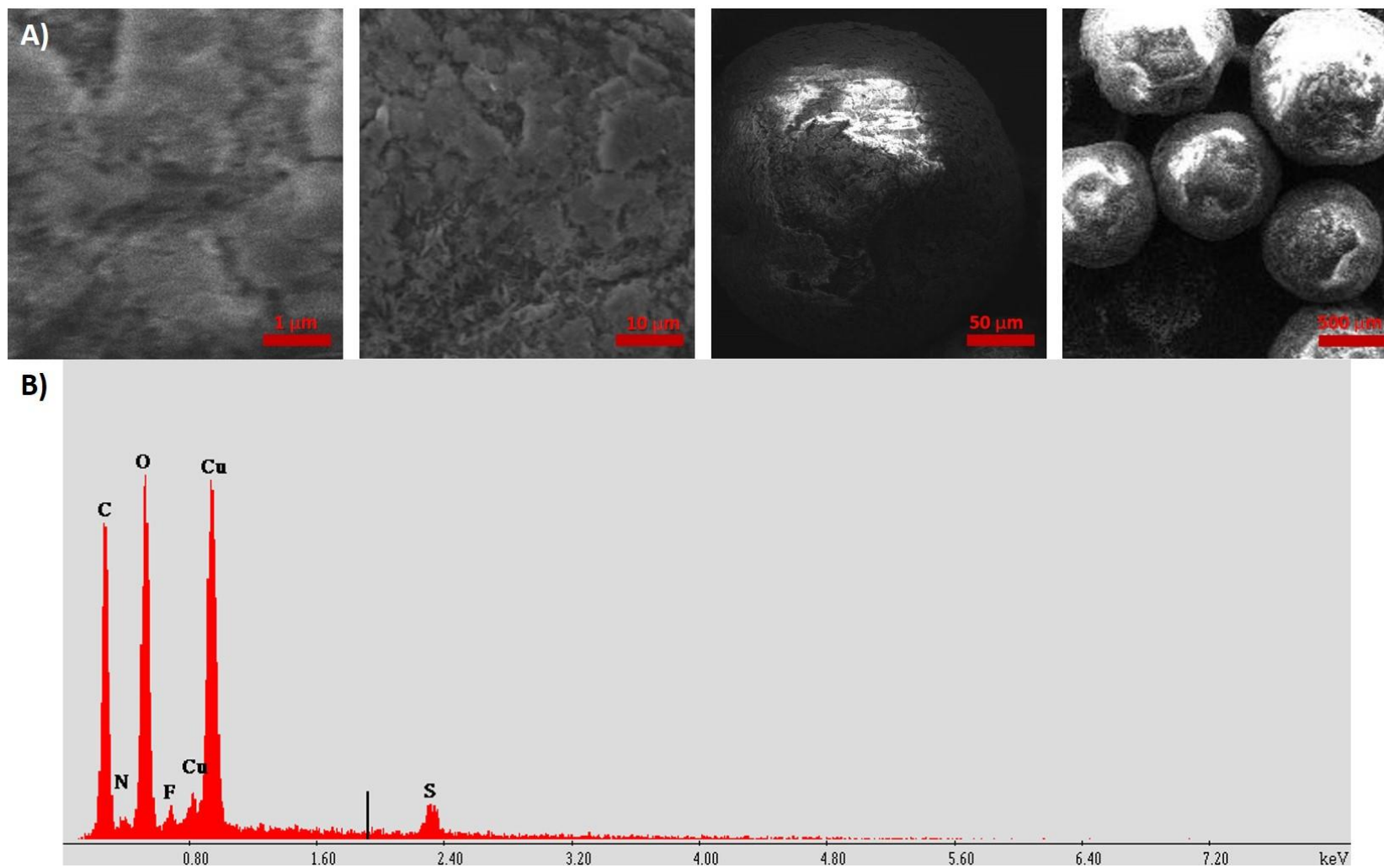


Figure 2.3.3 A) SEM images of PS-GHK-6-abx-Cu(II) complex, B) EDX Studies conforming the presence of Cu(II) on beads

immobilized on hydrophobic pockets provided by the alkyl tail of the molecule, so that they deployed closer to the active copper site of the catalyst. As a result, reaction yields increased at least two-fold. For the rest of the experiments, tert-butanol, methanol and water were used as they provided the highest activity.

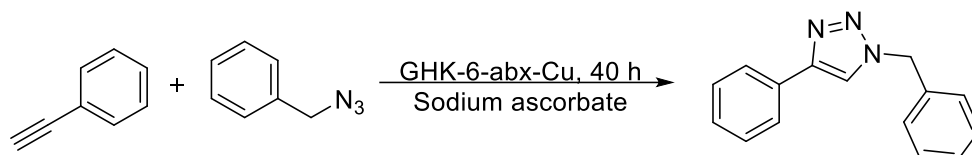


Figure 2.3.4 Schematic representation of click reaction between benzyl azide and phenyl acetylene

Solvent System (v/v)	% Yield
1:3 t-BuOH:H ₂ O	73 %
3:1 t-BuOH:H ₂ O	33 %
1:1 DMF:H ₂ O	26 %
1:1 MeOH:H ₂ O	70 %
1:1 ACN:H ₂ O	24 %

Table 2.3.3 Reaction yields of click reaction in different solvents, GHK-6-abx-Cu complex was used as catalyst, reaction proceed at 50 °C for 40 h

After the first run of the reaction, resin beads were recovered from the reaction mixture by filtration, washed and dried. To explore the presence of Cu(II) on beads before and after the reaction, X-Ray photoelectron spectroscopy (XPS) surveys were conducted on both GHK-6-abx (Figure 2.3.6) and GHK-11-adx (Figure 2.3.7) XPS analyses revealed the existance of Cu(II) for GHK-6-abx-Cu and GHK-11-adx-Cu both before and after usage. Cu 2p_{3/2} showed a peak at 934.7 eV.

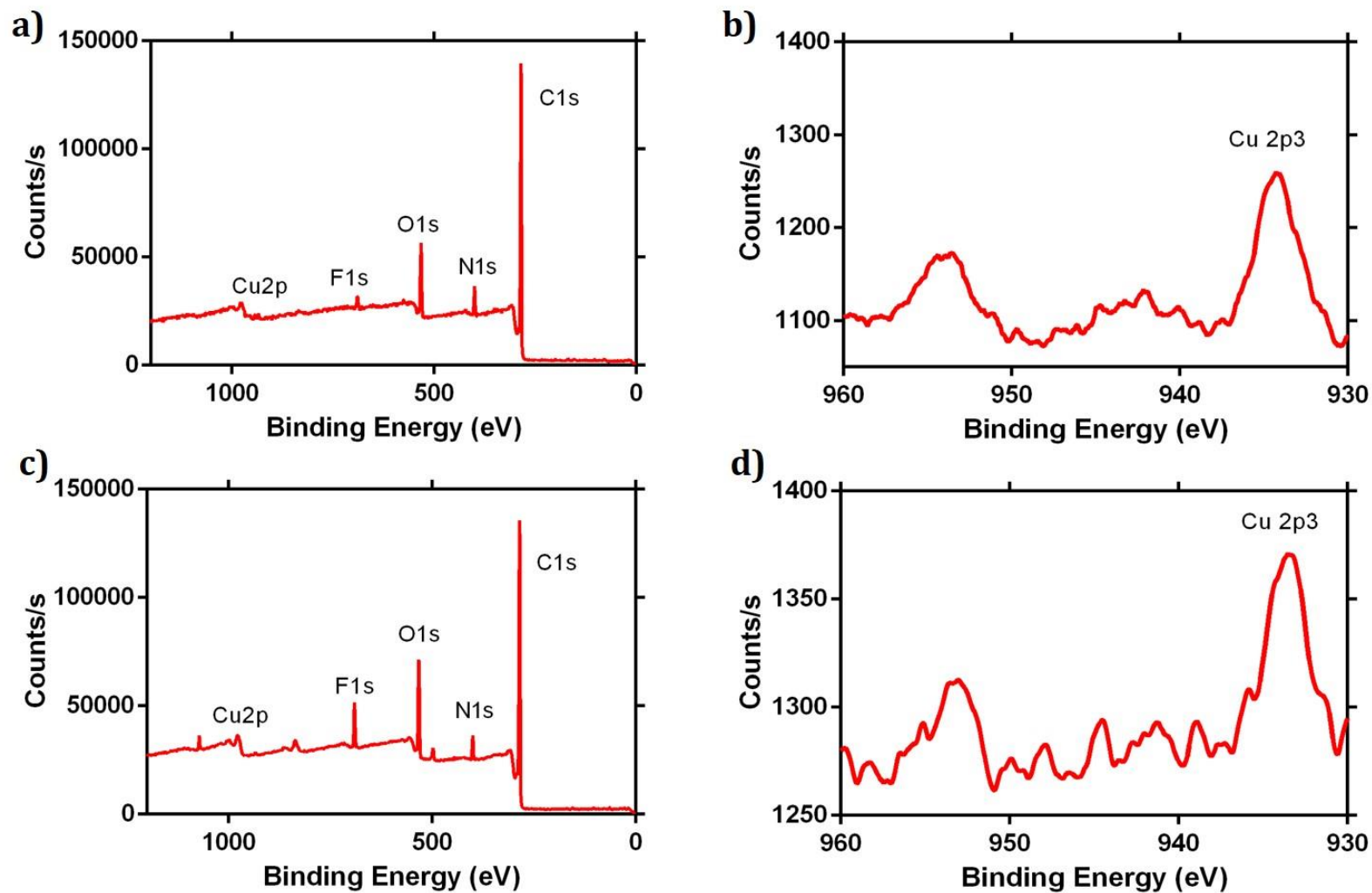


Figure 2.3.5 XPS Survey data of GHK-6-adx-Cu a) before usage, c) after usage, Cu survey data b) before usage, d) after usage (smoothing at polynomial 8)

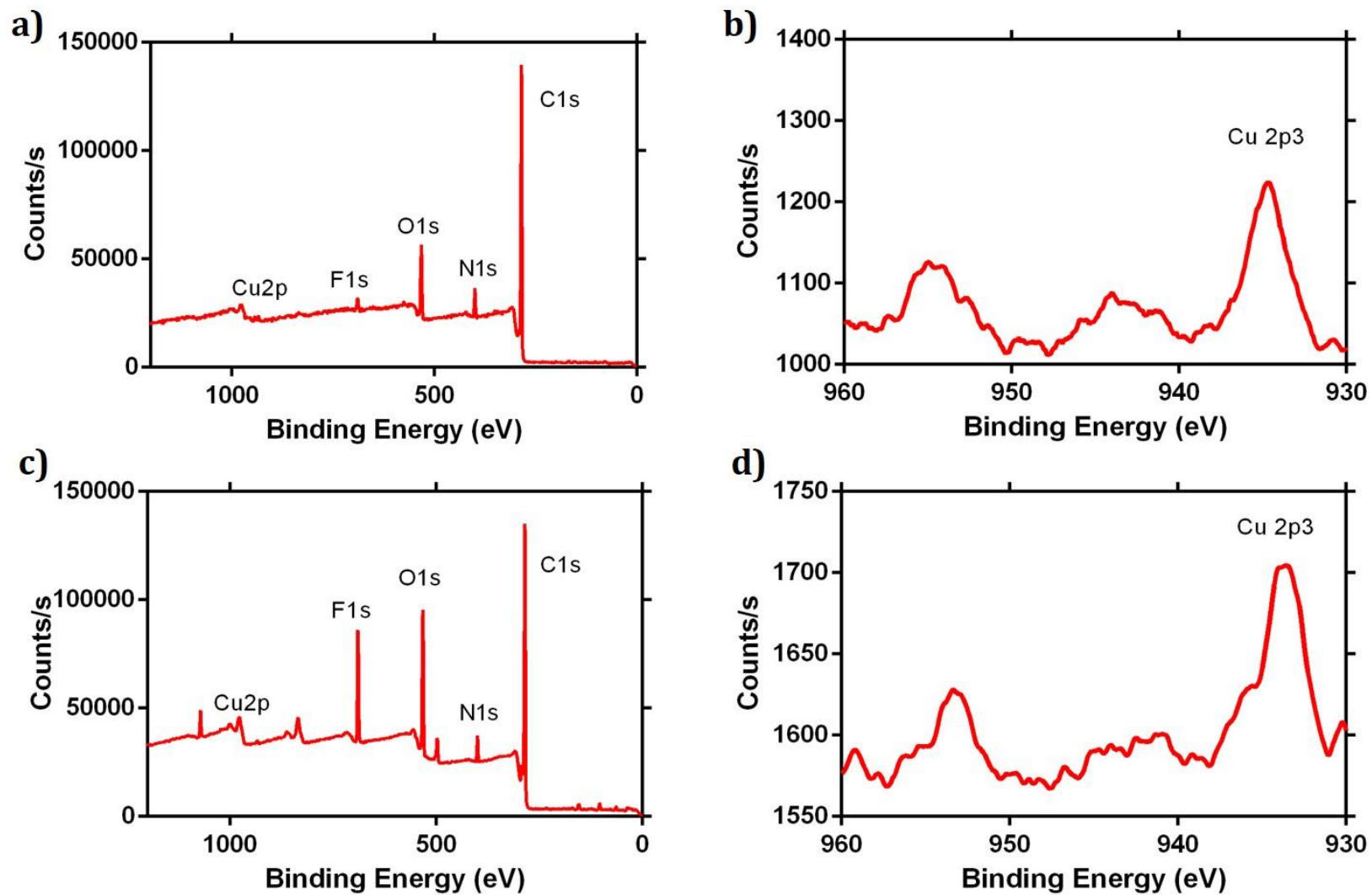


Figure 2.3.6 XPS Survey data of GHK-11-abx-Cu a) before usage, c) after usage, Cu survey data b) before usage, d) after usage (smoothing at polynomial 8)

For cross-validation, the presence of copper was investigated with UV-VIS before and after use. UV-VIS spectra of the catalyst, shown in Figure 2.3.8, were similar before and after use and exhibited an absorption peak around 650 nm, which is attributed to Cu²⁺-imidazole. Cu(II) was immobilized on the sequence by forming a complex with the imidazole moiety on histidine. XPS and UV-VIS results showed that the Cu(II) remains intact on the solid support and the catalyst is stable under the reaction conditions.

In order to test and compare the catalytic activities of the catalysts and to optimize solvent conditions, another set of reactions was carried out at 50 °C using t-butanol, methanol and water as solvents. Percentile yields obtained from the reactions are given in Table 2.3.2. Yields were overall higher for solvent systems containing higher percentages of water, due to the repulsion of organic reagents to the hydrophobic pockets of the catalyst by the hydrophilic environment provided by water. GHK-11-adx exhibited better catalytic activity in all solvent systems, potentially because of the longer alkyl chain of the molecule, which offers a more hydrophobic character for organic reagents. Recyclability is a key point for a heterogeneous catalyst. For this reason, following the recovery of the catalyst from the reaction mixture, catalytic activity of the recovered catalyst was investigated for a second run of the reaction. However, % yields were only as high as 21.3% for GHK-11-adx in 1:1 MeOH-H₂O solvent, which efficiently drove the reaction for the first run alone (93.4% yield). Although high yields were obtained under these conditions for the first run with very low loadings of the catalyst, recyclability of the catalysts was compromised; therefore, further optimization was required.

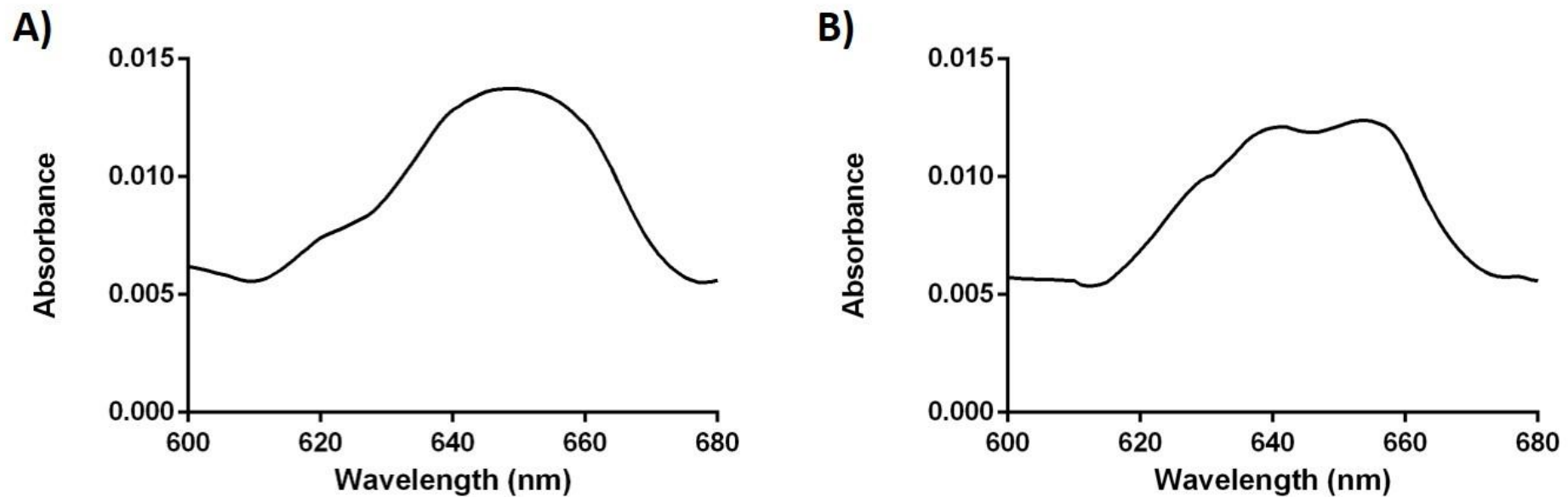


Figure 2.3.7 UV-VIS spectra of GHK-6-Cu catalyst in DMF A) before use, B) after use. An absorption peak around 650 nm which is assigned to Cu²⁺-imidazole complex.

	GHK-6-abx	GHK-11-adx
Solvent	% Yield	% Yield
1:1 MeOH-H ₂ O	72%	93%
1:1 t-BuOH-H ₂ O	30%	60%
1:3 t-BuOH-H ₂ O	69%	78%

Table 2.3.4 Reaction yields of click-reactions when GHK-6-abx-Cu complex and GHK-11-adx-Cu complex was used as the catalyst in different solvent systems.

Optimal conditions for both recyclability and high yields were established as 40 °C and an aqueous environment, whereafter the recyclability of the catalyst was explored. For this, a series of three successive runs under optimal conditions were carried out with both GHK-6-abx and GHK-11-abx. Results are shown in Table 2.3.3. GHK-11-adx-Cu complex afforded the highest efficiency in water at 80.1% yield. 1:1 MeOH-H₂O system is the close second in efficiency with 71.4% yield and offers the smallest drop in efficiency for further runs with only a 6% drop at the end of the third run. GHK-6-abx-Cu complex provided the highest efficiency in the 1:1 MeOH-H₂O system as well as the smallest drop in efficiency for consecutive runs, with an 11.9% drop at the end of the third run. In both of these cases, the 1:1 MeOH-H₂O solvent system provided the best recyclability for the reaction. The efficiency was the lowest for the H₂O environment for the reaction catalyzed by GHK-6-abx-Cu complex, probably resulting from the lack of a sufficiently hydrophobic environment for the reagents to dissolve and react with each other. Recyclability of the GHK-11-adx-Cu complex for the synthesis of 1-benzyl-4-phenyl-1H-1,2,3-triazole in water and 1:1 MeOH-H₂O is shown in Figure 2.3.9 Only a small reduction

in catalytic activity was observed following reuse, which was further confirmed by the presence of Cu(II) in XPS and UV-VIS analyses.

As a negative control, bare resin without GHK peptide sequence which went through the same copper complexation procedure with the GHK-6-abx and GHK-11-adx was prepared. Its catalytic activity was tested under the optimal conditions, 40°C and aqueous environment, towards click reaction. After 40 h, obtained % yield was lower than 5%. Thus, it can be concluded that catalytic activity of the system is resulted from the molecular design itself.

GHK-11-adx	1 st run	2 nd run	3 rd run
Solvent	% Yield	% Yield	% Yield
1:1 MeOH-H ₂ O	71%	68%	64%
3:1 t-BuOH-H ₂ O	64%	59%	52%
H ₂ O	80%	76%	69%
GHK-6-abx			
1:1 MeOH-H ₂ O	65%	60%	54%
3:1 t-BuOH-H ₂ O	54%	43%	38%
H ₂ O	41%	29%	26%

Table 2.3.5 Reaction yields of click-reactions when GHK-6-abx-Cu complex and GHK-11-adx-Cu complex was used as the catalysts in different solvent systems, at 40 °C, 40 h.

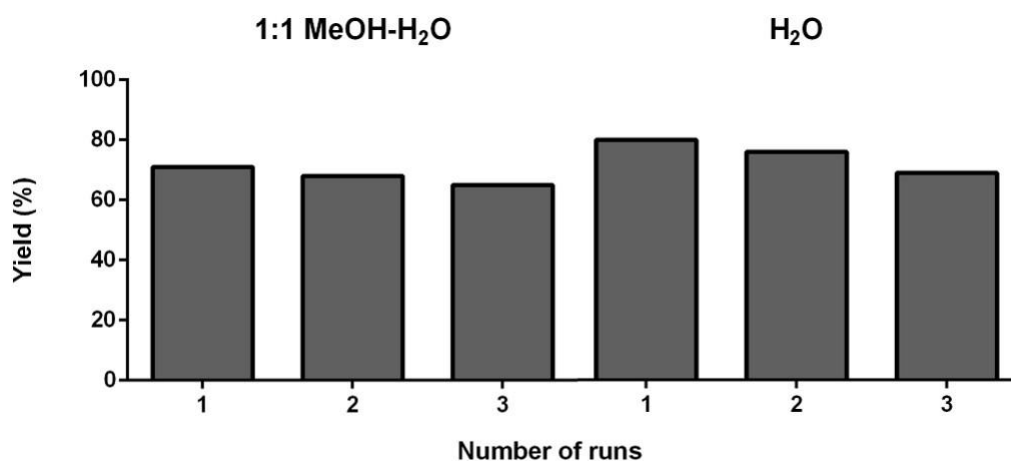


Figure 2.3.8 Recyclability of GKH-11-adx-Cu complex to afford 1,2,3 triazole product, at 40 °C for 40 h

Target 1-benzyl-4-phenyl-1H-1,2,3-triazole product was characterized with GC-MS, ¹H and ¹³C-NMR analyses. GC-MS chromatogram of an exemplary reaction mixture and MS data of the product is shown in Figure 2.3.9. MS (C₁₅H₁₃N₃)_{calculated} m/z is 235.29, MS(C₁₅H₁₃N₃)_{observed} m/z was 235.1.

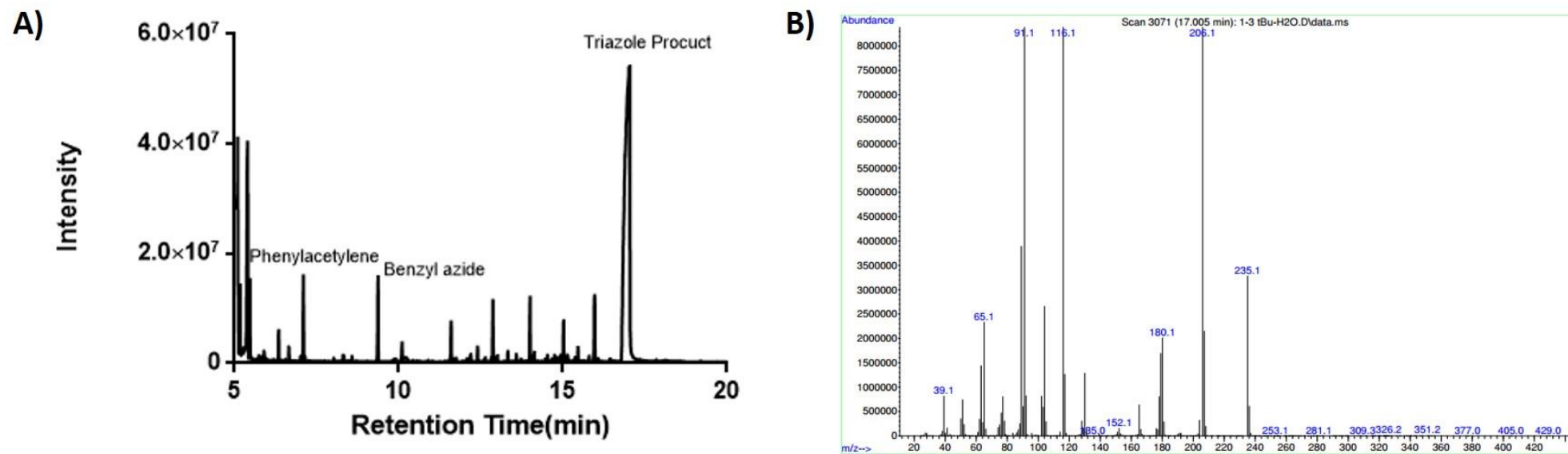


Figure 2.3.9 GC-MS analysis of 1-benzyl-4-phenyl-1H-1,2,3 A) Chromatogram of reaction mixture comprising 1:1 MeOH-H₂O, at 40 °C, after 40 h, B) Mass Spectrometry data of the product MS (C₁₅H₁₃N₃)_{calculated}=239.29, MS (C₁₅H₁₃N₃)_{observed}=235.1

The product was further characterized with NMR after the removal of EtOAc. Residual phenyl acetyne and benzyl azide was also removed during vacuum distillation process and the target product was obtained pure without any additional purification process. ^1H NMR (400 MHz, CDCl_3) δ (ppm)= 5.59 (s, 2 H), 7.28-7.35 (m, 3 H), 7.38-7.44 (m, 5 H), 7.68 (s, 1 H), 7.81-83 (d, 2 H); ^{13}C NMR (100 MHz, CDCl_3) δ (ppm)=54.22, 119.50, 125.71, 128.06, 128.16, 128.78, 128.80, 129.16, 130.57, 134.72, 148.23 (Figure 2.3.10)

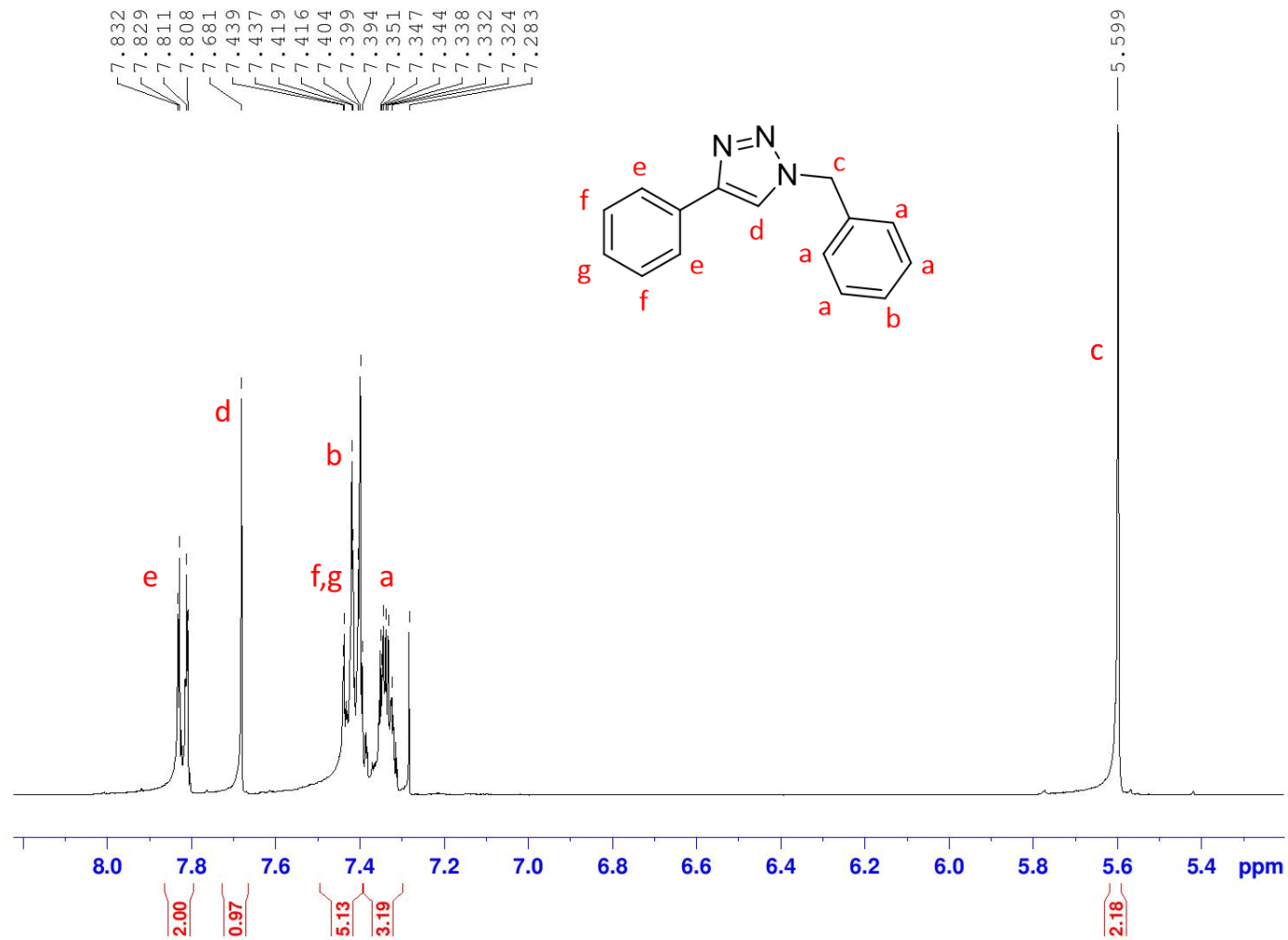


Figure 2.3.10 A. ¹H-NMR of 1-benzyl-4-phenyl-1H-1,2,3-triazole in CDCl₃

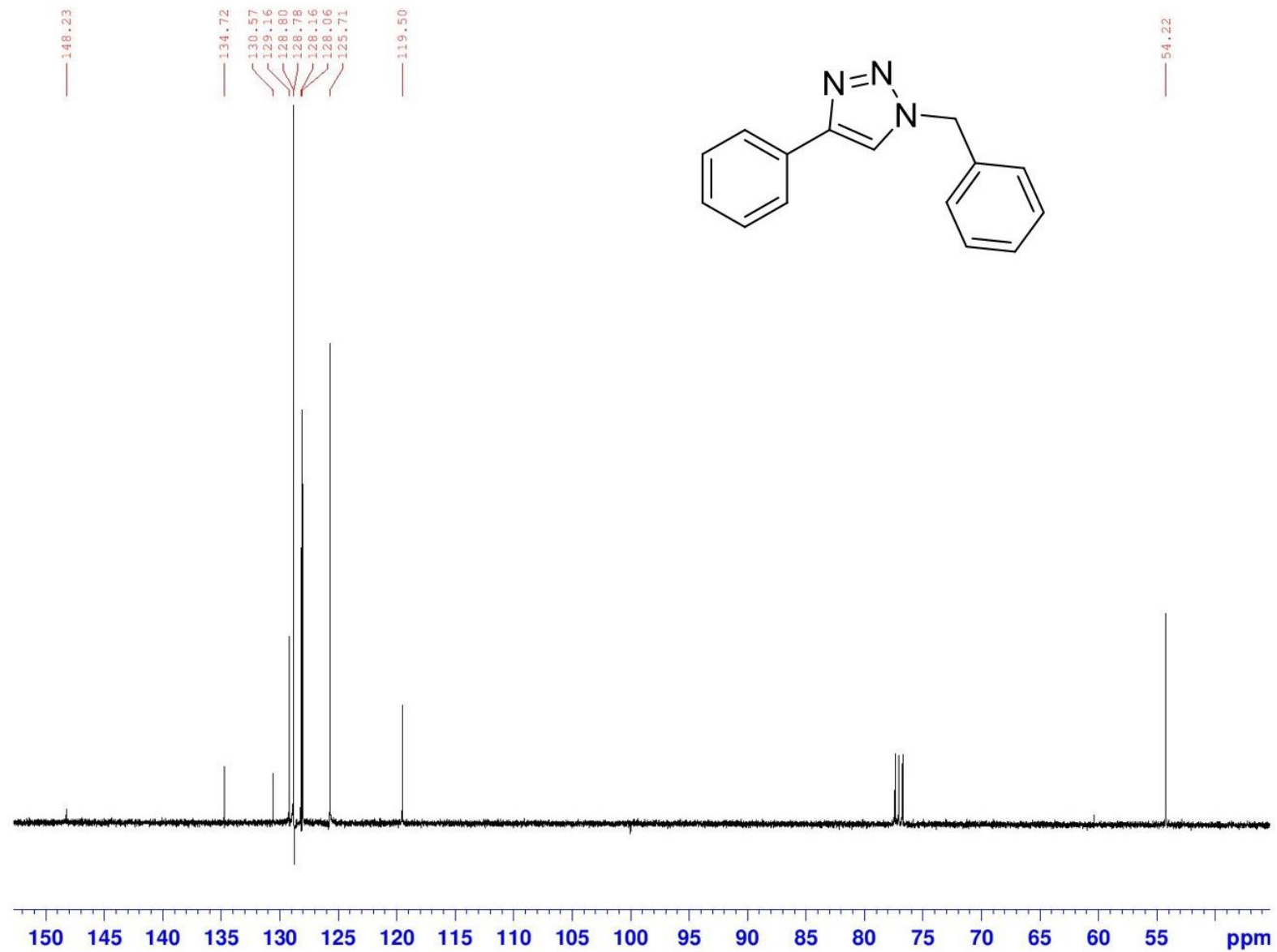


Figure 2.3.10 B. ^{13}C -NMR of 1-benzyl-4-phenyl-1H-1,2,3-triazole in CDCl_3

2.4. CONCLUSION

In the present study, I showed the development of a heterogeneous, recyclable, biomimetic peptide-based catalyst for [3+2] Huisgen cycloaddition reactions in water, which was found to be the ideal medium for the click reaction due to the hydrophobic and hydrophilic parts of the peptide sequence. GHK, a copper-binding peptide sequence, was connected to the Rink amide resin through an alkyl tail to provide the system with hydrophobic pockets, which allow the reaction to proceed by immobilizing reagents at positions close to the active sites of the catalyst. Consequently, the overall mechanism-of-action of the system is similar to enzyme catalysts, which facilitate reactions between organic reagents in an aqueous environment. Cu(II) amounts used for catalyzing reactions were as low as 0.005 mol equivalent, and the system could be reused at least three times without significant loss in catalytic activity. In addition, the polymer support further increased the efficiency of the catalyst by offering thermal stability and chemical inertness. We therefore believe that the peptide/resin catalyst presents a cost-effective and sustainable system that can easily be produced in the kg scale. The heterogeneous system is very attractive due to its facile and inexpensive method of synthesis, lack of waste byproducts, ability to function optimally at low reaction temperatures and compatibility with aqueous conditions, which fulfills all the hallmarks of an effective green chemistry reaction.

CHAPTER 3

PHOTORESPONSIVE SELF-ASSEMBLY OF PEPTIDE

AMPHIPHILES

3.1. INTRODUCTION

Peptide amphiphiles (PA) are surfactant agents that are composed of hydrophobic and hydrophilic molecular segments, exhibit the functions of bioactive peptides, and assemble into a variety of nanostructures.[138] PAs can form several secondary conformational structures due to π - π interactions, hydrophobic effects, electrostatic interactions and hydrogen bondings in the peptide. [139–142]

In nature, responsive peptide-based materials, like motor-proteins and enzymes, use a combination of these individually weak interactions. Consequently, these interactions collaborate in order to give dynamically organized secondary, tertiary and quaternary structures.[143] There exist a specific type of peptide amphiphile which is known to self-assemble into 1D nanostructures, mainly nanofibers with a cylindrical geometry, under physiological conditions.[138] There are several external factors affecting self-assembly of peptide amphiphiles such as PA concentrations, temperature, pH, length of hydrophobic segments and the salt concentrations.[144–153] A change in these properties simultaneously changes the assembly characteristics of the peptide amphiphiles; therefore, such a prompted change can be used to control self-assembly.

The ability to direct self-assembly behavior using switchable peptides is beneficial for many processes, including drug delivery applications, tissue engineering and biosensing.[154, 155] As such, many attempts have been devoted to the generation of smart (also called “intelligent”) materials which has the ability to alter their physical or biochemical properties with respect to external stimuli. It is possible to use light, pH and temperature changes, biochemical signals or electrical fields as stimuli for such purposes.[156–161] Photochemically responsive materials are more useful in

this context since they permit the use of light, which is a readily available, highly stable, versatile, easy to handle and cheap reagent.[162] Moreover, light-based systems allow more precise stimulation and provide quick responses. Manipulation of assembly in a quick manner is also possible using light as a stimulus.[162] Moreover, peptides are composed of a diverse range of amino acids that exhibit various properties and can easily be decorated with small organic molecules; as a result, it is rather easy to design these molecules to be photo-responsive.

Several examples of photo-triggered self-assembly and disassembly of peptide amphiphiles have been reported to date. These systems commonly employ the usage of either photo-removable protecting groups (“cages”) or photo-switchable azobenzene groups.

Photo-switchable azobenzene groups are commonly used in controlling the properties of compounds without physical contact. These photo-sensitizers change their configuration simultaneously and reversibly from trans to cis (or E- to Z-) when they are exposed to UV light. For example, Deeg *et al.* demonstrated a light-switchable azobenzene peptide which can aggregate into amyloidlike structures when the azobenzene chromophore AMPP ([3-(3-aminomethyl)phenylazo]phenylacetic acid) is in the trans-configuration.[163] Illumination of the aggregates causes trans-to-cis isomerization of AMPP, leading to local structural defects that cause disaggregation.[163] Azo-benzene chemistry provides a prominent approach for photo-triggered systems due to its status as a reversible process; however, preparation procedures for peptides bearing azo-benzene groups are very lengthy and challenging.

3.1.1 Cages

Photo-removable protecting groups (“cages”) are commonly used agents in organic chemistry and biology [164–167] Functional or reactive molecules which have become functionally or chemically inert by the covalent modification of the groups providing the functionality or the activity via a photo-removable protecting group, are defined with the term “caged”. [167] Upon irradiation, the protecting group can be cleaved from the molecule. Subsequently, cage release (“uncaging”), which is triggered with light, restores the molecular activity.[168]

In this scope, 2-nitro-benzyl groups are the most commonly used groups for photo-triggered assembly and disassembly of peptides, since they can be removed very easily and quickly upon irradiation. Bosques *et al.* reported a methodology that enables the temporal control of fibrilization of amyloid like peptides.[169] In this study, a photo-linker, 3-amino-3-(2-nitrophenyl)-propionic acid (ANP), and fibril inhibitory units, N,N-dimethyl-ethylenediamine (DMDA), are connected to the amyloid like peptide.[169]. As fibril inhibitory units, DMDA is removed from the peptide by photolysis, fibrilization occurs simultaneously.[169]. In another approach, Stupp *et al.* presented the transformation of higher order supramolecular architectures using light as a stimulus.[138] Accordingly, a peptide amphiphile molecule bearing a bulky photocleavable nitrobenzyl group which self-assembles into a quadruple helical fibers and when irradiated, it dissociates into single nonhelical fibrils.[138]

In all of the reported systems, the nitro-benzyl moiety is covalently attached to the peptide backbone, requiring synthesis of different peptide sequences from scratch

and making the preparation very lengthy, which in turn makes the method impractical and limits its usage in diverse applications.

Recently, different photo-labile calcium chelators (Ca^{2+} cages) were reported to exhibit a strong binding affinity towards Ca^{2+} ions, while releasing them upon irradiation due to irreversible changes in their molecular structure.[170, 171] Ca^{2+} is a divalent cation that does not interfere with the biocompatibility of the compounds, yet plays an important role in regulating many biological functions including muscle contraction, differentiation, biomineralization, nerve impulses and secretion.[172–175] Calcium cages are used to control biological functions by utilizing light to trigger Ca^{2+} release and subsequently stimulate biological responses.

Here we report, a general strategy for the use of a photolabile calcium chelator, Nitr-T, for triggering the ion-mediated self-assembly of negatively charged peptide amphiphiles. Ca^{2+} is known to induce self-assembly by ionic cross-linking with the side chain of glutamic acid (E) residues on the PA molecule. Mechanical properties of the PA improve with the presence of free Ca^{2+} ions in the medium, resulting in gelation and the formation of a hydrogel. No covalent modification of the PA molecule is required in this process. We therefore provide a modular approach for light-triggered self-assembly and tuning of swelling and mechanical properties of any PA molecule bearing negatively-charged side chains.

3.2. EXPERIMENTAL SECTION

3.2.1. Materials

All manipulations and experiments were conducted under atmospheric pressure and at room temperature unless otherwise noted. Water was deionized in Milli Q water

purifier system. Rink amide MBHA resin (0.78 mmol/g loading), all Fmoc-protected amino acids, lauric acid, diisopropylethylamine (DIEA) and *N,N,N',N'*-tetramethyl-O-(1*H*-benzotriazole-1-yl) uronium hexafluorophosphate (HBTU) were purchased from Merck Milipore, Novabiochem. Calcium cage, Nitr-T was kindly provided by Prof. Aránzazu del Campo (Germany). All the other solvents, acids, reagents, acids and bases used were in analytical grade, and used without further purification and were purchased from the commercial suppliers, Invitrogen, Fisher, Merck, Alfa Aesar, and/or Sigma-Aldrich.

3.2.2. Peptide-Amphiphile Synthesis, Characterization and Purification

Lauryl-VVAGEE-Am (E₂) PA was synthesized on MBHA Rink Amide resin on 0.5 mol scale using standard Fmoc based solid phase peptide synthesis. Amino acid couplings were done by mixing 2 equivalents of Fmoc-protected amino acid 3 equivalents of DIEA and 1.95 equivalents of HBTU in dimethylformamide (DMF) for 1 equivalent of ring amide resin and shaking the mixture for 4 h. After each coupling, uncoupled N-terminal amine was acetylated in 10% acetic anhydride-DMF solution by shaking the resin for 30 min to prevent formation of byproducts. Fmoc groups were removed by shaking the reaction vessel with 20% piperidine/dimethylformamide (DMF) solution for 20 min. Following each step, the resin was washed thoroughly three times with dimethylformamide (DMF), then three times with dichloromethane (DCM) and subsequently three times with dimethylformamide (DMF) again. After completion of all couplings, resin was washed thoroughly with DCM and PA molecules were cleaved from the resin by treating the resin with 95% trifluoro-acetic acid (TFA) cleavage cocktail comprising TFA: TIS: H₂O in the ratio of 95: 2.5: 2.5 for 2.5 hours. Afterwards, resin washed

with DCM very carefully and washing solution containing the peptide was collected. DCM and remaining TFA were removed by using vacuum distillation. The remaining viscous peptide solution was triturated through the following steps: Around 200 mL of ice cold ether (-20 °C) was added on the obtained product following the removal of solvent and TFA, kept overnight at -20 °C. Then, ether was separated from the peptide by ultracentrifugation at 8500 rpm for 25 min. Following the trituration, peptide was dissolved in 0.1% NH₄OH-water solution and freeze-dried.

3.2.2.1. Liquid Chromatography- Mass Spectrometry (LC-MS)

In order to characterize PA molecules and check their purity, an Agilent Technologies 6530 Accurate-Mass Q-TOF LC-MS equipped with an Electron Spray Ionization (ESI) source was utilized. The concentration of the sample was 1 mg/mL. 0.1% NH₄OH-water and 0.1%NH₄OH-acetonitrile solutions were used as eluents.

3.2.2.2. Preparative High Performance Liquid Chromatography (Prep-HPLC)

The peptide molecules were purified by utilizing reverse phase prep-HPLC technique. 0.1% NH₄OH-water and 0.1%NH₄OH-acetonitrile solutions were used as eluents. Volume fraction of acetonitrile was increased from 2% to 70% within 30 min at a solvent flow 20 mL/min. An Agilent 1200 HPLC equipped with an Agilent Zorbax Extend-C18 (50 x 2.1 mm) column and a Q-TOF ESI-MS was used. After collecting the fractions containing the pure peptide, acetonitrile was removed by *vacuo* and water was removed by freeze-drying. Peptide product was collected as a white powder.

3.2.3. Nuclear Magnetic Resonance (NMR)

Bruker Ultra Shield-250 MHz was used for NMR analysis. 2.0 mg of the Nitr-T, synthesized as reported in Ref. [170], was dissolved in 0.7 mL of DMSO-*d*₆ with tetramethyl silane (TMS) as internal standard. All measurements were done at 25 °C, chemical shifts were given as ppm.

3.2.4. High Performance Liquid Chromatography (HPLC)

HPLC analysis of Nitr-T was performed by using Jasco HPLC 2000 with a diode array UV-VIS detector. As eluents, 0.1% TFA-water and 5% water-0.1% TFA-acetonitrile solutions were used. Runs were performed at a solvent flow of 1 mL/min. The volume fraction of acetonitrile was increased from 5% to 95% within 30 min.

3.2.5. Ca²⁺-Nitr-T Complex Formation

The 8.4 mg of Nitr-T (0.01 mmol, 861.2 g/mol) was dissolved in 80 μL, 0.5 M NaOH solution. To this, 1.06 g of CaCl₂ (0.01 mmol, 110.2 g/mol) was added and the resulting mixture was sonicated for 2 h at 50 °C for Ca²⁺-Nitr-T complex to form. The mixture kept at dark to prevent any unwanted photolysis of photolabile Nitr-T molecule.

3.2.6. Preparations of Hydrogels

As control groups, 2.0 wt % E₂ solutions were prepared by dissolving the the E₂ in basic water. 2 wt % E₂-cage solution was prepared by the addition of 14.0 mg of E₂ peptide in 80 μL Nitr-T solution and dilution of this mixture to 700 μL by water addition. Viscosity of the resulting solution was similar of the original 2.0 wt % E₂ solution. E₂/Ca²⁺ hydrogels were prepared by mixing the 1 mM CaCl₂ solutions with 4.0 wt % E₂ solution at 1:1 ratio.

3.2.7. Rheological Analyses

An Anton Paar MCR-301 Rheometer was used. 90 μL of the samples were loaded to PP12-SN17979 measuring device with 12 mm diameter. Time sweep tests of each sample were carried out for 20 min. Angular frequency and strain magnitudes were adjusted as $\omega=10$ rad/s and $\gamma=0.1\%$, respectively. Measuring distance was 0.5 mm. UV-triggered gelation of E₂-cage mixtures were tested by placing 90 μL of 2 wt % E₂/Nitr-T on the rheometer's plate in a homemade humidity chamber that prevents the samples from drying out during UV exposure, and treating the sample with 365 nm UV-light for 30 min followed with incubation for 10 min in the dark for the stabilization of the sample. To destroy hydrogels formed due to UV exposure, 10 μL of 1 wt % EDTA was added and mixed with the hydrogel prior to the measurements.

3.3. RESULTS AND DISCUSSION

Nitr-T molecule is a photo-labile calcium chelator that has high affinity towards Ca²⁺ ions and when treated with 365 nm UV light; it photolyzes to release free Ca²⁺ ions to the medium.[170] Both this process and the molecular structure of Nitr-T is shown in Figure 3.3.1.A. Lauryl-VVAGEE (E₂-PA) is a negatively charged PA; of which chemical representation is shown in Figure 3.1.B was synthesized by using standard Fmoc-based peptide synthesis. Since E₂-PA is a negatively charged PA molecule, it self-assembles in the presence of free Ca²⁺ ions released by the photolysis of the Nitr-T-Ca²⁺ complex and produces a hydrogel scaffold. This process is illustrated in Figure 3.3.1.C.

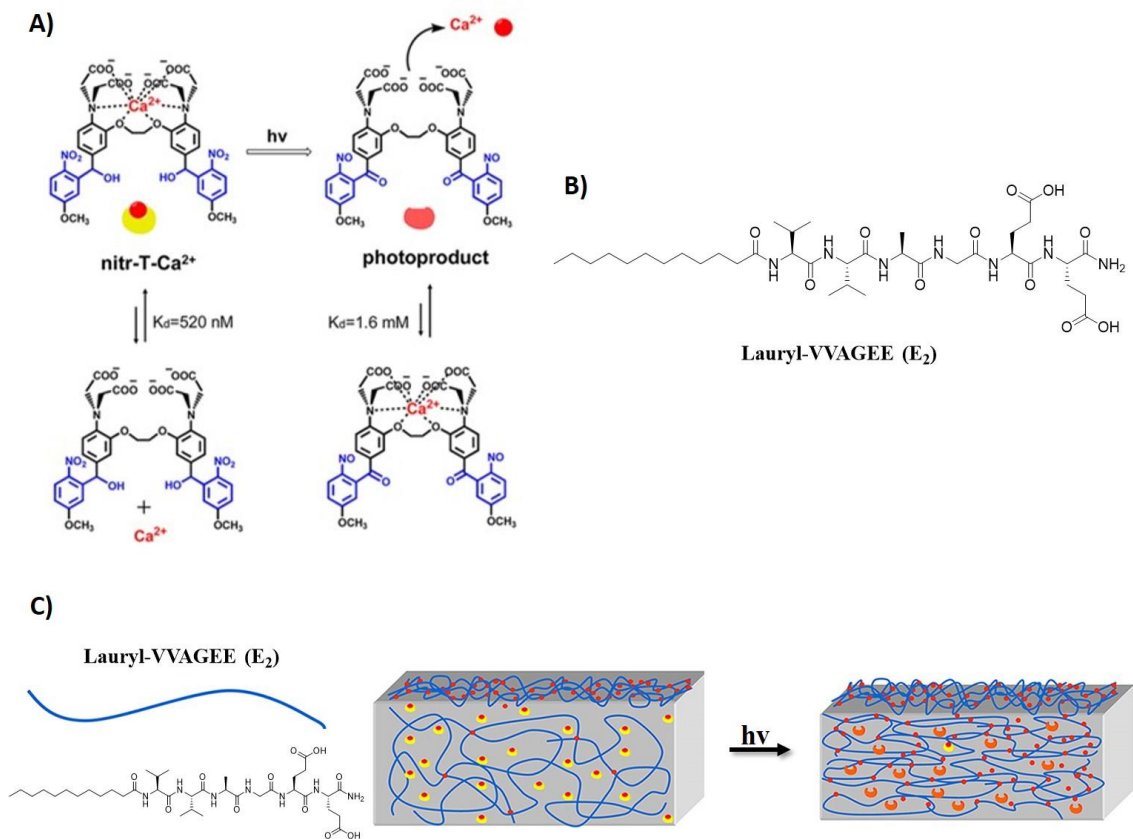


Figure 3.3.1 A) Molecular structure of Nitr-T molecule, before and after photolysis, Nitr-T- Ca^{2+} complex. Adapted with permission from Ref.[176] Copyright (2016) American Chemical Society B) Chemical representation of Lauryl-VVAGEE-Am PA (E_2 -PA) C) Schematic representation of photo-triggered gelation of E_2 -PA with Nitr-T.

Following its synthesis E_2 -PA was purified with HPLC and then characterized with LC-MS (Figure 3.3.2). MS ($\text{C}_{37}\text{H}_{65}\text{N}_7\text{O}_{11}\text{-H}^-$): 782.42 (Calculated was m/z 782.92, observed was m/z 782.42)

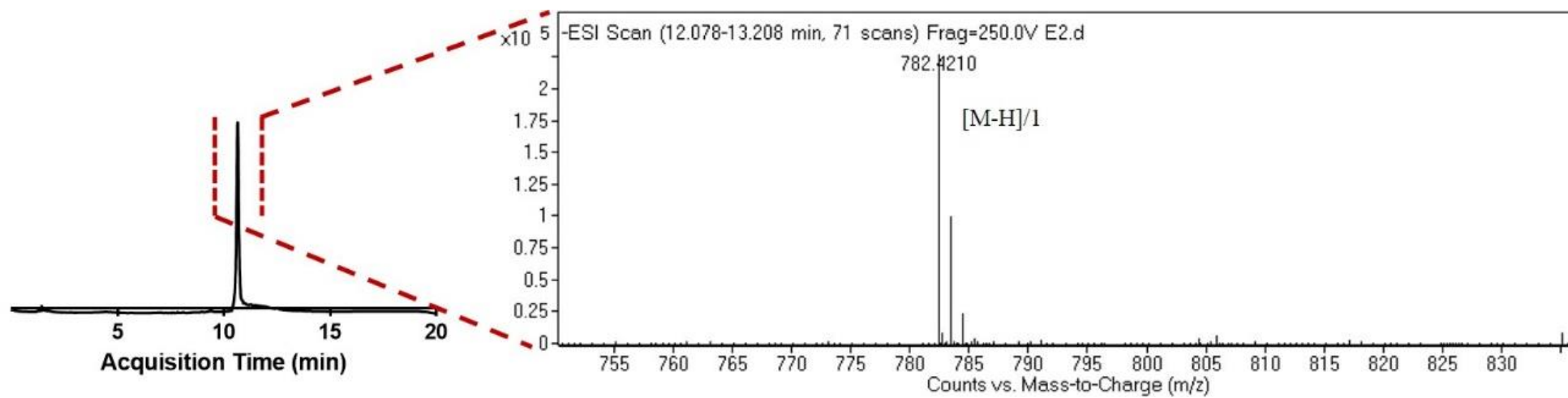


Figure 3.3.2 Liquid Chromatography-Mass Spectrometry (LC-MS) analyses of E₂-PA

1,2-Bis{2-amino-5-[(5-methoxy-2-nitrophenyl)hydroxymethyl]-phenoxy} ethane-N,N,N',N'-tetraacetic acid (Nitr-T tetraethyl ester) was characterized with $^1\text{H-NMR}$. (DMSO- d_6 , 250 MHz) δ ppm = 8.003–7.99 (dd, 2H), 7.38–7.36 (d, 2H), 7.03–7.01 (d, 2H), 6.93 (s, 2H), 6.72–6.63 (m, 4H), 6.25 (s, 2H), 4.19 (s, 4H), 4.019 (s, 8H), 3.866 (s, 6H) (Figure 3.3.4)

In order to observe gelation behavior and to test the mechanical properties of the E₂-PA-Ca²⁺ gel, the same amount of calcium that will theoretically be released upon 30 min of UV irradiation ($K_d = 1.6$ mM, 75% photo-conversion) was mixed with E₂-PA and rheological analyses were conducted on the resulting mixture.[176] The PA solution was found to form a hydrogel immediately after the introduction of CaCl₂ solution which can be observed macroscopically. Results of the analysis are shown in Figure 3.3.3.

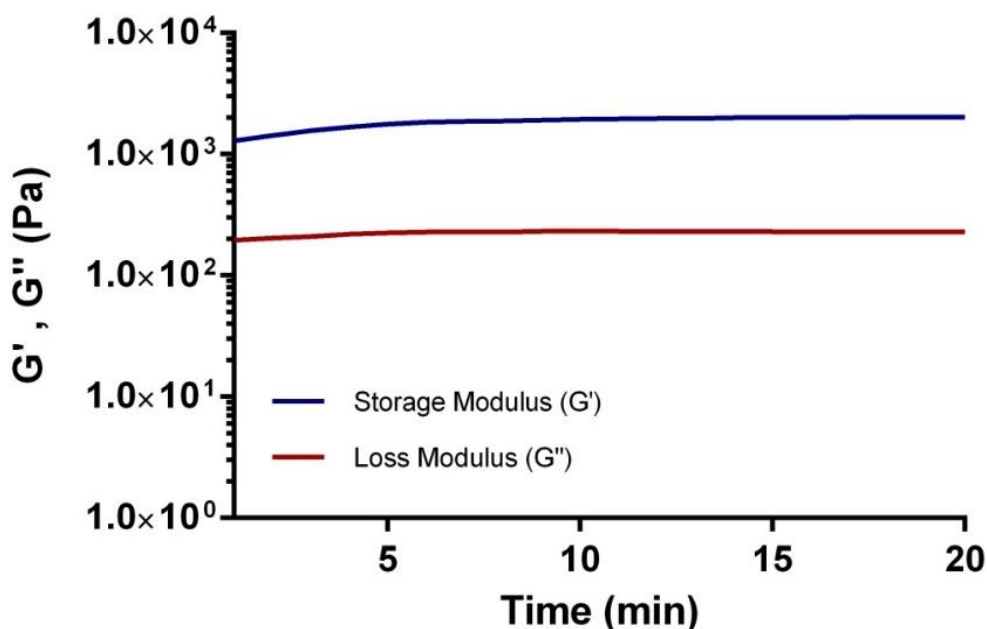


Figure 3.3.3 Rheological analysis of 2 wt % E₂-PA-Ca²⁺ gel

A supplementary series of rheological analyses were then conducted to demonstrate that the hydrogel formation is triggered in the presence of free Ca^{2+} ions in the medium and not by any other stimuli (Figure 3.3.5). Hydrogels, which are viscoelastic materials, are characterized by higher storage modulus values than loss modulus values. The storage modulus of the material comes from its gel character, while loss modulus is related to the viscosity of the sample. 2 wt % E₂-PA solution itself behaved as water and demonstrated a storage modulus of 0, showing that the PA itself does not behave as a gel. To show that the, neither presence of Nitr-T; or formed photo-products of Nitr-T and/or the irradiation process do not trigger the gelation of E₂-PA, the PA solution was mixed with Nitr-T compound before complexing it with Ca^{2+} and the mechanical properties of the resulting mixture were investigated with rheological analyses before and after UV treatment.

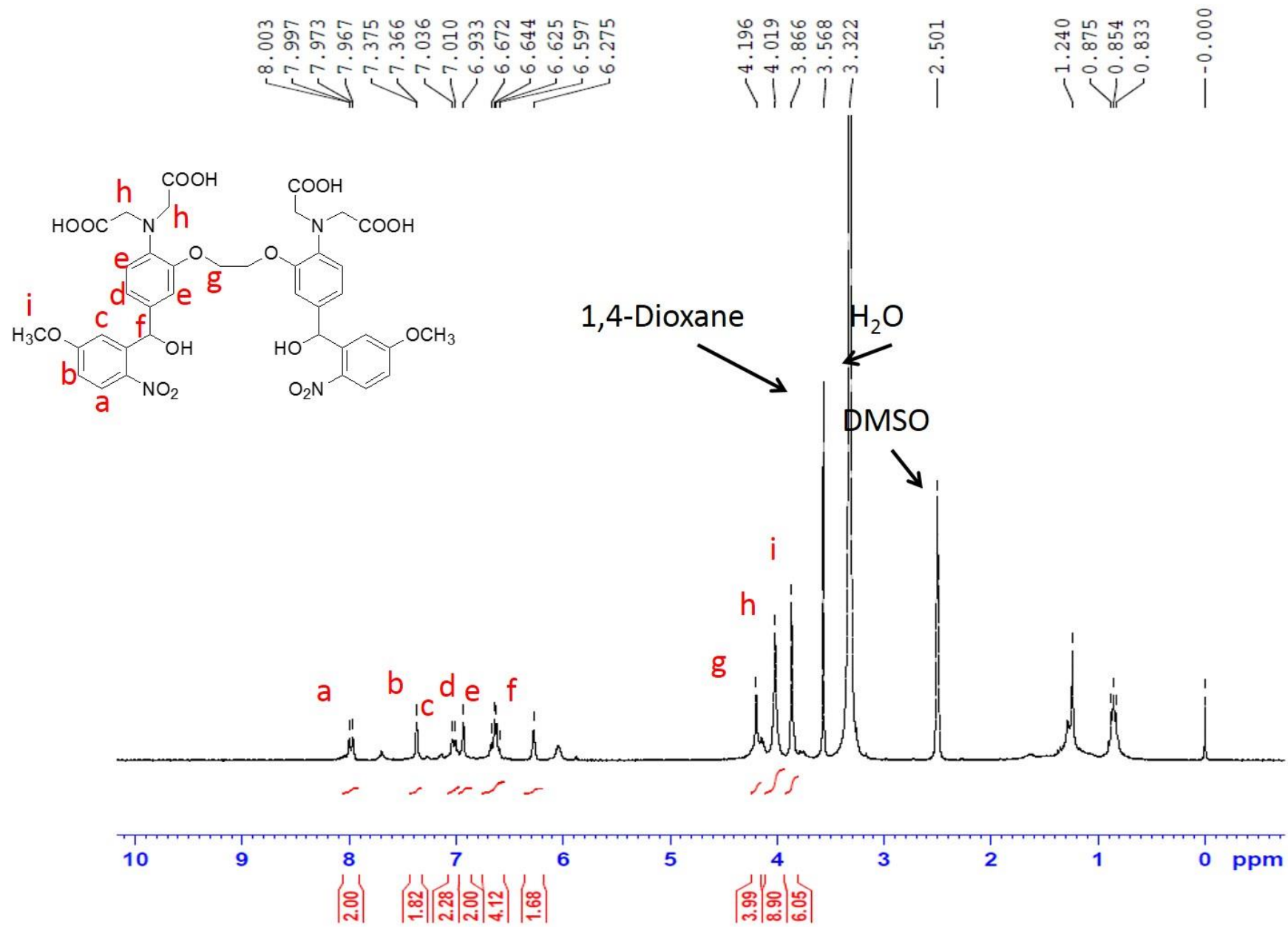


Figure 3.3.4 ¹H-NMR Spectrum of Nitr-T tetraethyl ester

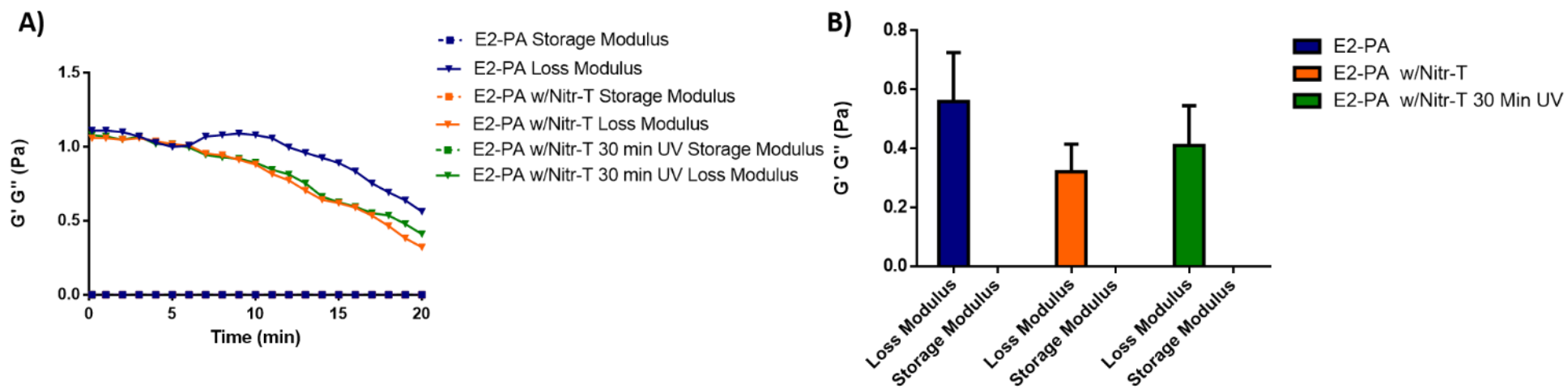


Figure 3.3.5 Rheological analyses of only 2.0 wt % E₂-PA, E₂-PA w/Nitr-T and E₂-PA w/Nitr-T after 30 minutes of UV treatment B) Modulus values with error bars collected from the samples at t=20 min, N=3.

Photo-triggerable hydrogel formation from E₂-PA/Nitr-T-Ca²⁺ mixture is illustrated in Figure 3.3.6.A. In part I of Figure 3.3.6, before UV- treatment, the mixture is in solution phase. After 30 min of UV-treatment, the mixture forms a hydrogel as shown in Figure 3.3.6.A part II. Following the addition of 1 wt % EDTA solution to the hydrogel, system goes back to the solution state. Rheological analyses were conducted to test the mechanical properties of the samples (Figure 3.3.6.B). In part I, no storage modulus value was obtained from the sample, indicating that the sample behaves like a solution. After irradiation, as shown in part II, the sample demonstrates a very high storage modulus value compared to its loss modulus value, proving that the sample behaves as a hydrogel. Subsequent addition of the EDTA solution, facilitates the removal of free Ca²⁺ ions from the system and results in its reversion to the solution state as only loss modulus is observed for the sample (Figure 3.3.6.B, part III). As the removal of free Ca²⁺ ions from the medium causes E₂-PA to lose its gel behavior. it can be concluded that the gelation of E₂-PA results only from the presence of free Ca²⁺ ions.

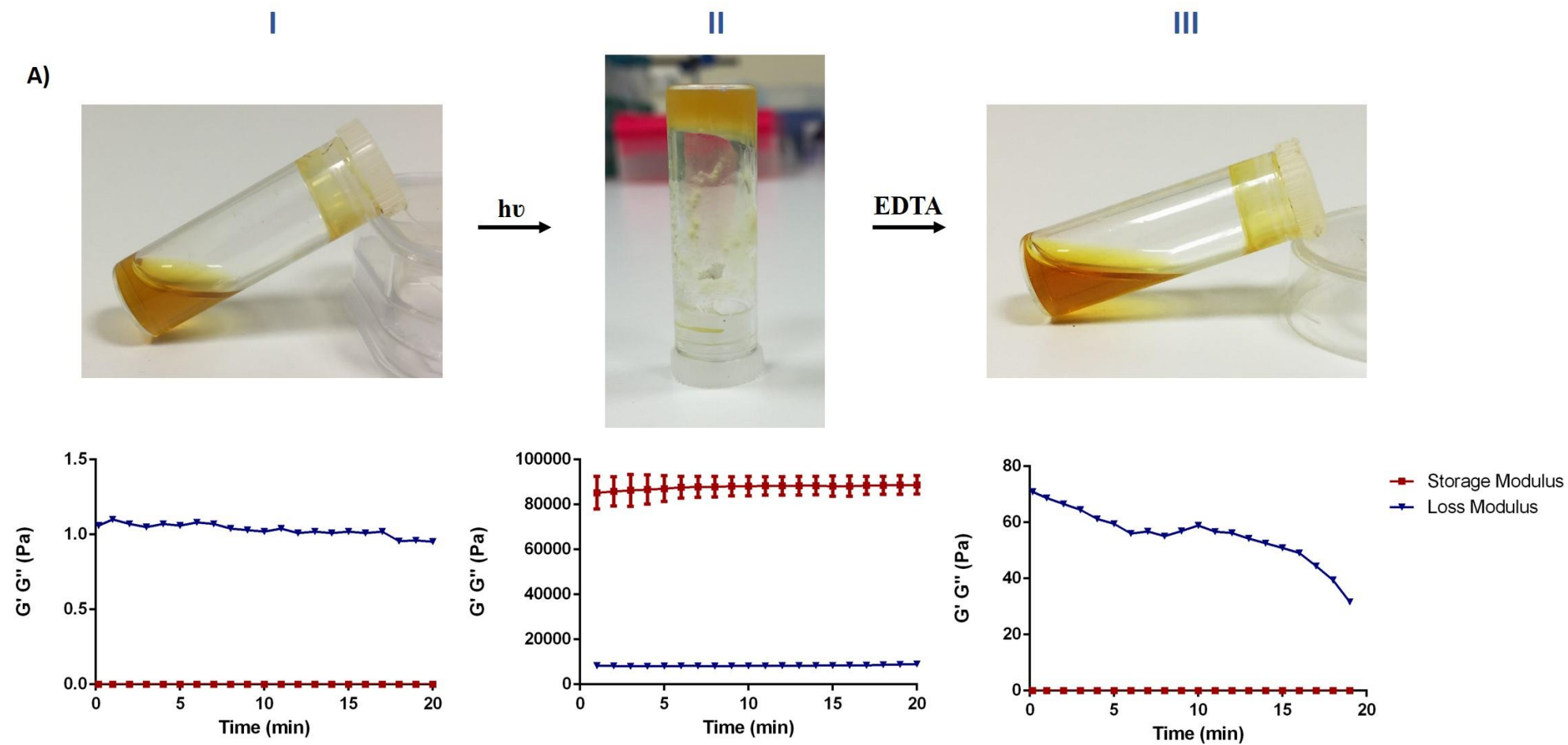


Figure 3.3.6 A) Photographs of photo-triggerable 2 wt % E₂-PA/Nitr-T-Ca²⁺ hydrogel system I. before irradiation, in solution state II. After 30 min of UV-irradiation, in hydrogel state III. after the addition of 1 wt% EDTA solution, in solution state. B) Results of rheological analyses of the corresponding samples shown in part A, N=2.

3.4. CONCLUSION

In this study, reversible photo-triggerable self-assembly of a negatively charged PA molecule, E₂-PA, was illustrated for the first time in the absence of any covalent modifications. Nitr-T, a photo-labile calcium cage, was complexed with Ca²⁺ and utilized as a calcium source for the E₂-PA molecule, which forms a hydrogel when free calcium ions are present in the medium. Through rheology measurements, we showed that the self-assembly of the E₂-PA is stimulated only by presence of free Ca²⁺ ions and can be regulated through irradiation. This study represents a proof of concept for controlling the self-assembly, swelling and mechanical properties of any system comprising negatively charged PAs through the introduction of a photo-labile calcium molecule, and has the potential to be widely applicable in drug delivery, regenerative medicine and tissue engineering purposes.

CHAPTER 4

CONCLUSION & FUTURE PROSPECTS

Bioinspired or biomimetic materials hold great importance in materials science in overcoming existing challenges and disadvantages as they enable development of new systems or processes inspired from nature's approaches for building highly complex and functional structures which can perform difficult and complicated tasks. In that sense, peptides provide a very attractive platform for developing new synthetic systems which can imitate complex protein functions, yet themselves are easy to produce since they are simple structures compared to proteins.

In the first study, a biomimetic heterogeneous copper complex catalyst was developed for [3+2] Huisgen cycloaddition reactions by utilizing a human tripeptide, GHK, with high affinity towards copper species.[3] In this design, GHK sequence was linked via an alkyl tail comprising six or eleven carbons to a polystyrene ring amide resin which acts as solid support providing thermal and chemical stability. This enables the addition of hydrophobic pockets to the molecule which compels organic reagents in aqueous environment, solubilizes them and keeps them closer to the catalytic active site of the molecule. Both the working principle and the recyclability of the catalyst is similar to the enzyme catalysis. By using the catalyst in water, up to 80% reaction yield can be achieved with Cu(II) loadings that are as low as 0.5 mol % for up to at least three cycles with a very small drop in catalytic activity. As mentioned, the highest efficiencies were obtained in aqueous solvents containing pure water or water-alcohol mixtures rather than organic solvents, which in fact is a very crucial prospect in point of green chemistry. Additionally, lack of requirement for removing copper species in the reaction product, is a simple yet effective way of producing the catalyst. In addition, the simple isolation procedure for the target product significantly reduces the length of the process and amount of

the supplementary products used for the process which subsequently reduces the cost. A cost-effective, environment friendly and easy to produce catalytic system is reported in the scope of the project.

Peptide amphiphiles (PA) are surfactant molecules which are composed of hydrophobic and hydrophilic segments and are known to assemble into a variety of nanostructures. Self-assembly of peptide the amphiphiles can be triggered by a variety of stimuli such as enzymes, ions, pH, heat, sonication, and light. In the second study, a versatile and modular system to control self-assembly of peptide-amphiphiles by using light as a stimulus was described. In order to accomplish that, a photo-labile calcium chelator which releases Ca^{2+} ions to the medium upon irradiation was simply mixed with a negatively charged peptide amphiphile molecule, E₂-PA, which self-assembles to form a hydrogel in the presence of free Ca^{2+} ions. In the described system, it was shown as a proof of concept that swelling and mechanical properties of the negatively charged PA solutions can be tuned by using light as an external stimulus in a reversible manner. Previously reported light-triggered self-assembling systems involved lengthy and complicated procedures where covalent modification of the molecules were required. However, no such procedure is required for the described system were that can be applied for light-triggered self-assembly of any negatively charged PA. This method can be widely applicable for many biological applications especially for tissue engineering as it presents a modular approach and calcium cages are commercially available.

The studies described in this thesis show the wide range of applicability of peptide-based bioinspired functional materials in material science to overcome previously reported problems and challenges by means of using simple yet effective ways.

Peptides can mimic the nature's approach in performing complicated tasks by using complex protein structures and adapt this approach in new material applications. As such, peptide based materials have the potential to revolutionize bioinspired materials field by their simplistic approaches.

Bibliography

- [1] L. A. Estroff and A. D. Hamilton, “At the interface of organic and inorganic chemistry: Bioinspired synthesis of composite materials,” *Chem. Mater.*, vol. 13, no. 10, pp. 3227–3235, 2001.
- [2] B. I. Technologies, *Biomimetics: biologically inspired technologies*, vol. 9, no. 3. 2006.
- [3] L. Pickart, “The human tri-peptide GHK and tissue remodeling,” *J. Biomater. Sci. Polym. Ed.*, vol. 19, no. 8, pp. 969–88, 2008.
- [4] C. Ortiz and M. Boyce, “Bioinspired structural materials,” *Science (80-.)*, vol. 14, no. February, pp. 1053–1054, 2008.
- [5] B. Hinnemann *et al.*, “Biomimetic Hydrogen Evolution: {MoS}₂ Nanoparticles as Catalyst for Hydrogen Evolution,” *J. Am. Chem. Soc.*, vol. 127, no. 15, pp. 5308–5309, 2005.
- [6] S. Deville, E. Saiz, R. K. Nalla, and A. P. Tomsia, “Freezing as a path to build complex composites,” *Science*, vol. 311, no. 5760, pp. 515–518, 2006.
- [7] E. Munch *et al.*, “Tough, bio-inspired hybrid materials,” *Science (80-.)*, vol. 322, no. 5907, pp. 1516–1520, 2008.
- [8] Z. Tang, N. a Kotov, S. Magonov, and B. Ozturk, “Nanostructured artificial nacre,” *Nat. Mater.*, vol. 2, no. 6, pp. 413–418, 2003.
- [9] E. P. Chan, C. Greiner, E. Arzt, and A. J. Crosby, “Designing model systems

- for enhanced adhesion,” *MRS Bull.*, vol. 32, no. June, pp. 496–503, 2007.
- [10] B. K. Ahn *et al.*, “High-performance mussel-inspired adhesives of reduced complexity,” *Nat. Commun.*, vol. 6, p. 7, 2015.
- [11] B. P. Lee, P. B. Messersmith, J. N. Israelachvili, and J. H. Waite, “Mussel-Inspired Adhesives and Coatings,” *Annu. Rev. Mater. Res.*, vol. 41, pp. 99–132, 2011.
- [12] A. Jagota, C. Y. Hui, N. J. Glassmaker, and T. Tang, “Mechanics of bioinspired and biomimetic fibrillar interfaces,” *MRS Bull.*, vol. 32, no. 6, pp. 492–495, 2007.
- [13] A. R. Parker and H. E. Townley, “Biomimetics of photonic nanostructures,” *Nat. Nanotechnol.*, vol. 2, pp. 347–353, 2007.
- [14] M. Nune, P. Kumaraswamy, U. M. Krishnan, and S. Sethuraman, “Self-assembling peptide nanofibrous scaffolds for tissue engineering: novel approaches and strategies for effective functional regeneration,” *Curr. Protein Pept. Sci.*, vol. 14, no. 1, pp. 70–84, 2013.
- [15] H. Geckil, F. Xu, X. Zhang, S. Moon, and U. Demirci, “Engineering hydrogels as extracellular matrix mimics,” *Nanomedicine (Lond.)*, vol. 5, no. 3, pp. 469–84, 2010.
- [16] A. Mata *et al.*, “Bone regeneration mediated by biomimetic mineralization of a nanofiber matrix,” *Biomaterials*, vol. 31, no. 23, pp. 6004–6012, 2010.
- [17] W. Y. Seow and C. A. E. Hauser, “Short to ultrashort peptide hydrogels for

- biomedical uses,” *Materials Today*, vol. 17, no. 8. pp. 381–388, 2014.
- [18] S. Fukuzumi, “Development of bioinspired artificial photosynthetic systems.,” *Phys. Chem. Chem. Phys.*, vol. 10, no. 17, pp. 2283–2297, 2008.
- [19] X. Yang, J. Zhu, L. Qiu, and D. Li, “Bioinspired effective prevention of restacking in multilayered graphene films: Towards the next generation of high-performance supercapacitors,” *Adv. Mater.*, vol. 23, no. 25, pp. 2833–2838, 2011.
- [20] D. Larcher and J.-M. Tarascon, “Towards greener and more sustainable batteries for electrical energy storage.,” *Nat. Chem.*, vol. 7, no. 1, pp. 19–29, 2015.
- [21] W. Chen, D.-K. Han, K.-D. Ahn, and J.-M. Kim, “Molecularly imprinted polymers having amidine and imidazole functional groups as an enzyme-mimetic catalyst for ester hydrolysis,” *Macromol. Res.*, vol. 10, no. 2, pp. 122–126, 2013.
- [22] A. Biswas, I. S. Bayer, A. S. Biris, T. Wang, E. Dervishi, and F. Faupel, “Advances in top-down and bottom-up surface nanofabrication: Techniques, applications & future prospects,” *Advances in Colloid and Interface Science*, vol. 170, no. 1–2. pp. 2–27, 2012.
- [23] Q. Xu, R. M. Rioux, M. D. Dickey, and G. M. Whitesides, “Nanoskiving: A new method to produce arrays of nanostructures,” *Accounts of Chemical Research*, vol. 41, no. 12. pp. 1566–1577, 2008.
- [24] J. T. Fourkas, “Nanoscale photolithography with visible light,” *J. Phys. Chem.*

- Lett.*, vol. 1, no. 8, pp. 1221–1227, 2010.
- [25] R. Nagpal, “Programmable Self-Assembly: Constructing Global Shape using Biologically-inspire,” *Dspace.Mit.Edu*, no. June, 2001.
- [26] S. Zhang, “Fabrication of novel biomaterials through molecular self-assembly,” *Nat. Biotechnol.*, vol. 21, no. 10, pp. 1171–1178, 2003.
- [27] J. Aizenberg, “Crystallization in patterns: A bio-inspired approach,” *Advanced Materials*, vol. 16, no. 15 SPEC. ISS. pp. 1295–1302, 2004.
- [28] E. Dujardin and S. Mann, “Bio-inspired materials chemistry,” *Adv. Mater.*, vol. 14, no. 11, pp. 775–788, 2002.
- [29] M. L. Curri, R. Comparelli, M. Striccoli, and a Agostiano, “Emerging methods for fabricating functional structures by patterning and assembling engineered nanocrystals,” *Phys. Chem. Chem. Phys.*, vol. 12, no. 37, pp. 11197–11207, 2010.
- [30] X. Zhao, F. Pan, and J. R. Lu, “Recent development of peptide self-assembly,” *Prog. Nat. Sci.*, vol. 18, no. 6, pp. 653–660, 2008.
- [31] W. F. Daamen, J. H. Veerkamp, J. C. M. van Hest, and T. H. van Kuppevelt, “Elastin as a biomaterial for tissue engineering,” *Biomaterials*, vol. 28, no. 30. pp. 4378–4398, 2007.
- [32] A. Mitra, J. Mulholland, A. Nan, E. McNeill, H. Ghandehari, and B. R. Line, “Targeting tumor angiogenic vasculature using polymer-RGD conjugates,” *J. Control. Release*, vol. 102, no. 1, pp. 191–201, 2005.

- [33] C. Walsh, "Enabling the chemistry of life.," *Nature*, vol. 409, no. January, pp. 226–231, 2001.
- [34] U. B. Sleytr, E. M. Egelseer, N. Ilk, D. Pum, and B. Schuster, "S-Layers as a basic building block in a molecular construction kit," *FEBS Journal*, vol. 274, no. 2, pp. 323–334, 2007.
- [35] M. B. Dickerson, K. H. Sandhage, and R. R. Naik, "Protein- and peptide-directed syntheses of inorganic materials," *Chem. Rev.*, vol. 108, no. 11, pp. 4935–4978, 2008.
- [36] Y. Ikezoe *et al.*, "Peptide-Metal Organic Framework Swimmers that Direct the Motion toward Chemical Targets," *Nano Lett.*, vol. 15, no. 6, pp. 4019–4023, 2015.
- [37] G. Gulseren, I. C. Yasa, O. Ustahuseyin, E. D. Tekin, A. B. Tekinay, and M. O. Guler, "Alkaline phosphatase-mimicking peptide nanofibers for osteogenic differentiation," *Biomacromolecules*, vol. 16, no. 7, pp. 2198–2208, 2015.
- [38] M. A. Khalily, O. Ustahuseyin, R. Garifullin, R. Genc, and M. O. Guler, "A supramolecular peptide nanofiber templated Pd nanocatalyst for efficient Suzuki coupling reactions under aqueous conditions," *Chem. Commun.*, vol. 48, no. 92, pp. 11358–11360, 2012.
- [39] M. J. Krysmann, S. S. Funari, E. Canetta, and I. W. Hamley, "The effect of PEG crystallization on the morphology of PEG/peptide block copolymers containing amyloid ??-peptide fragments," *Macromol. Chem. Phys.*, vol. 209, no. 9, pp. 883–889, 2008.

- [40] C. L. Chen and N. L. Rosi, "Peptide-based methods for the preparation of nanostructured inorganic materials," *Angewandte Chemie - International Edition*, vol. 49, no. 11. pp. 1924–1942, 2010.
- [41] A. Ghorbani-Choghamarani and Z. Taherinia, "Synthesis of peptide nanofibers decorated with palladium nanoparticles and its application as an efficient catalyst for the synthesis of sulfides via reaction of aryl halides with thiourea or 2-mercaptobenzothiazole," *RSC Adv.*, vol. 6, no. 64, pp. 59410–59421, 2016.
- [42] I. Maity, D. B. Rasale, and A. K. Das, "Peptide nanofibers decorated with Pd nanoparticles to enhance the catalytic activity for C–C coupling reactions in aerobic conditions," *RSC Adv.*, vol. 4, no. 6, pp. 2984–2988, 2014.
- [43] T. T. Lee *et al.*, "Light-triggered in vivo activation of adhesive peptides regulates cell adhesion, inflammation and vascularization of biomaterials.," *Nat. Mater.*, vol. 14, no. 3, pp. 352–60, 2015.
- [44] I. A. Banerjee, L. Yu, and H. Matsui, "Cu nanocrystal growth on peptide nanotubes by biomineralization: size control of Cu nanocrystals by tuning peptide conformation.," *Proc. Natl. Acad. Sci. U. S. A.*, vol. 100, no. 25, pp. 14678–82, 2003.
- [45] W. M. Pardridge, "Vector-mediated peptide drug delivery to the brain," *Advanced Drug Delivery Reviews*, vol. 15, no. 1–3. pp. 109–146, 1995.
- [46] Y. Loo, A. Lakshmanan, M. Ni, L. L. Toh, S. Wang, and C. A. E. Hauser, "Peptide Bioink: Self-Assembling Nanofibrous Scaffolds for Three-

- Dimensional Organotypic Cultures,” *Nano Lett.*, vol. 15, no. 10, pp. 6919–6925, 2015.
- [47] R. Djalali, Y. F. Chen, and H. Matsui, “Au nanocrystal growth on nanotubes controlled by conformations and charges of sequenced peptide templates,” *J. Am. Chem. Soc.*, vol. 125, no. 19, pp. 5873–5879, 2003.
- [48] L. Yu, I. A. Banerjee, and H. Matsui, “Direct Growth of Shape-Controlled Nanocrystals on Nanotubes via Biological Recognition,” *J. Am. Chem. Soc.*, vol. 125, no. 48, pp. 14837–14840, 2003.
- [49] K. S. Lee and J. R. Parquette, “A self-assembled nanotube for the direct aldol reaction in water,” *Chem. Commun.*, vol. 51, no. 86, pp. 15653–15656, 2015.
- [50] O. S. Makin, E. Atkins, P. Sikorski, J. Johansson, and L. C. Serpell, “Molecular basis for amyloid fibril formation and stability,” *Proc. Natl. Acad. Sci. U. S. A.*, vol. 102, no. 2, pp. 315–320, 2005.
- [51] C. E. Semino, J. R. Merok, G. G. Crane, G. Panagiotakos, and S. Zhang, “Functional differentiation of hepatocyte-like spheroid structures from putative liver progenitor cells in three-dimensional peptide scaffolds,” *Differentiation*, vol. 71, no. 4–5, pp. 262–270, 2003.
- [52] T. C. Holmes, S. de Lacalle, X. Su, G. Liu, a Rich, and S. Zhang, “Extensive neurite outgrowth and active synapse formation on self-assembling peptide scaffolds,” *Proc. Natl. Acad. Sci. U. S. A.*, vol. 97, no. 12, pp. 6728–6733, 2000.
- [53] B. M. Trost, “Selectivity: a key to synthetic efficiency.,” *Science (80-.)*, vol.

- 219, no. 4582, pp. 245–250, 1983.
- [54] B. M. Trost, “The Atom Economy - A Search for Synthetic Efficiency,” *Science* (80-.), vol. 254, no. 5037, pp. 1471–1477, 1991.
- [55] B. M. Trost, “Atom Economy—A Challenge for Organic Synthesis: Homogeneous Catalysis Leads the Way,” *Angew. Chemie Int. Ed. English*, vol. 34, no. 3, pp. 259–281, 1995.
- [56] R. A. Sheldon, “Atom efficiency and catalysis in organic synthesis*,” *Pure Appl. Chem. Pure Appl. Chem*, vol. 72, no. 7, pp. 1233–1246, 2000.
- [57] V. Polshettiwar, C. Len, and A. Fihri, “Silica-supported palladium: Sustainable catalysts for cross-coupling reactions,” *Coordination Chemistry Reviews*, vol. 253, no. 21–22, pp. 2599–2626, 2009.
- [58] B. M. Trost, “Basic Aspects of Organic Synthesis with Transition Metals.,” *Transit. Met. Org. Synth.*, vol. 1, pp. 3–14, 2004.
- [59] F. D. A. de Meijere, *Metal-Catalyzed Cross-Coupling Reactions*. 2008.
- [60] D. C. Harrowven, “Handbook of Organopalladium Chemistry for Organic Synthesis,” *Synthesis (Stuttg)*, vol. 2003, no. 4, pp. 632–632, 2003.
- [61] R. J. P. Corriu and J. P. Masse, “Activation of Grignard reagents by transition-metal complexes. A new and simple synthesis of trans-stilbenes and polyphenyls,” *J. Chem. Soc. Chem. Commun.*, p. 144a, 1972.
- [62] J. C. Shi, X. Zeng, and E. I. Negishi, “Highly selective synthesis of (E)-3-methyl-1-trialkylsilyl-3-en-1-yne via trans-selective alkynylation catalyzed

- by $\text{Cl}_2\text{Pd}(\text{DPEphos})$ and stereospecific methylation with methylzincs catalyzed by $\text{Pd}(\text{tBu } 3\text{P})_2$,” *Org. Lett.*, vol. 5, no. 11, pp. 1825–1828, 2003.
- [63] Q. Wang and C. Chen, “Nickel-catalyzed carbonylative Negishi cross-coupling reactions,” *Tetrahedron Lett.*, vol. 49, no. 18, pp. 2916–2921, 2008.
- [64] J. P. Wolfe, R. A. Singer, B. H. Yang, and S. L. Buchwald, “Highly active palladium catalysts for Suzuki coupling reactions,” *J. Am. Chem. Soc.*, vol. 121, no. 41, pp. 9550–9561, 1999.
- [65] T. Hatakeyama *et al.*, “Iron-catalyzed Suzuki-Miyaura coupling of alkyl halides,” *J. Am. Chem. Soc.*, vol. 132, no. 31, pp. 10674–10676, 2010.
- [66] K. Sonogashira, “Development of Pd-Cu catalyzed cross-coupling of terminal acetylenes with sp^2 -carbon halides,” *J. Organomet. Chem.*, vol. 653, no. 1–2, pp. 46–49, 2002.
- [67] M. C. Daniel and D. Astruc, “Gold Nanoparticles: Assembly, Supramolecular Chemistry, Quantum-Size-Related Properties, and Applications Toward Biology, Catalysis, and Nanotechnology,” *Chemical Reviews*, vol. 104, no. 1, pp. 293–346, 2004.
- [68] J. K. Stille, “The Palladium-Catalyzed Cross-Coupling Reactions of Organotin Reagents with Organic Electrophiles,” *Angew. Chemie Int. Ed.*, vol. 25, pp. 508–524, 1986.
- [69] N. Miyaura and A. Suzuki, “Palladium-Catalyzed Cross-Coupling Reactions,” *Chemistry*, vol. 95, no. 1, pp. 2457–2483, 1995.

- [70] K. Dooleweerd, B. P. Fors, and S. L. Buchwald, "Pd-catalyzed cross-coupling reactions of amides and aryl mesylates," *Org. Lett.*, vol. 12, no. 10, pp. 2350–2353, 2010.
- [71] J. P. Nolley and R. F. Heck, "Palladium-catalyzed vinylic hydrogen substitution reactions with aryl, benzyl, and styryl halides," *J. Org. Chem.*, vol. 37, no. 14, pp. 2320–2322, 1972.
- [72] H. Alper, J. B. Woell, B. Despeyroux, and D. J. H. Smith, "The regiospecific palladium catalysed hydrocarboxylation of alkenes under mild conditions," *J. Chem. Soc. Chem. Commun.*, no. 21, p. 1270, 1983.
- [73] C. Botteghi, S. Paganelli, L. Bigini, and M. Marchetti, "Hydroformylation of 1-aryl-1-(2-pyridyl)ethenes catalyzed by rhodium complexes," *J. Mol. Catal.*, vol. 93, no. 3, pp. 279–287, 1994.
- [74] G. Vasapollo, A. Somasunderam, B. El Ali, and H. Alper, "Synthesis of unsaturated acids by 1,2-addition of formic acid to conjugated dienes catalyzed by palladium on carbon in the presence of mono and bidentate phosphines," *Tetrahedron Lett.*, vol. 35, no. 34, pp. 6203–6206, 1994.
- [75] Y. Duan, L. Li, M. W. Chen, C. Bin Yu, H. J. Fan, and Y. G. Zhou, "Homogenous Pd-catalyzed asymmetric hydrogenation of unprotected indoles: Scope and mechanistic studies," *J. Am. Chem. Soc.*, vol. 136, no. 21, pp. 7688–7700, 2014.
- [76] K. H. Park, S. U. Son, and Y. K. Chung, "Sequential actions of palladium and cobalt nanoparticles immobilized on silica: One-pot synthesis of bicyclic

- enones by catalytic allylic alkylation and Pauson-Khand reaction,” *Org. Lett.*, vol. 4, no. 24, pp. 4361–4363, 2002.
- [77] M. Haruta, “Catalysis of gold nanoparticles deposited on metal oxides,” *CATTECH*, vol. 6, no. 3, pp. 102–115, 2002.
- [78] B. H. Lipshutz and B. R. Taft, “Heterogeneous copper-in-charcoal-catalyzed click chemistry,” *Angew. Chemie - Int. Ed.*, vol. 45, no. 48, pp. 8235–8238, 2006.
- [79] R. L. Oliveira, P. K. Kiyohara, and L. M. Rossi, “High performance magnetic separation of gold nanoparticles for catalytic oxidation of alcohols,” *Green Chem.*, vol. 12, p. 144, 2010.
- [80] W. Baker, R Thomas and Tumas, “Toward greener chemistry,” *Science (80-.)*, vol. 284, pp. 1477--1479, 1999.
- [81] D. J. Cole-Hamilton, “Homogeneous Catalysis--New Approaches to Catalyst Separation, Recovery, and Recycling,” *Science (80-.)*, vol. 299, no. 5613, pp. 1702–1706, 2003.
- [82] R. B. Nasir Baig and R. S. Varma, “A highly active magnetically recoverable nano ferrite-glutathione-copper (nano-FGT-Cu) catalyst for Huisgen 1,3-dipolar cycloadditions,” *Green Chem.*, vol. 14, no. 3, p. 625, 2012.
- [83] J. Lahann, *Click Chemistry for Biotechnology and Materials Science*. 2009.
- [84] E. Ozkal, S. Özçubukçu, C. Jimeno, and M. a. Pericàs, “Covalently immobilized tris(triazolyl)methanol–Cu(I) complexes: highly active and

- recyclable catalysts for CuAAC reactions,” *Catal. Sci. Technol.*, vol. 2, no. 1, p. 195, 2012.
- [85] J. M. Thomas and W. J. Thomas, *Principles and Practice of Heterogeneous Catalysis*, vol. 70, no. 5. 1997.
- [86] H. Bönemann, W. Brijoux, a Schulze Tilling, and K. Siepen, “Application of heterogeneous colloid catalysts for the preparation of fine chemicals,” *Top. Catal.*, vol. 4, pp. 217–227, 1997.
- [87] S. Minakata and M. Komatsu, “Organic reactions on silica in water,” *Chemical Reviews*, vol. 109, no. 2. pp. 711–724, 2009.
- [88] M. Chtchigrovsky *et al.*, “Functionalized chitosan as a green, recyclable, biopolymer-supported catalyst for the [3+2] huisgen cycloaddition,” *Angew. Chemie - Int. Ed.*, vol. 48, no. 32, pp. 5916–5920, 2009.
- [89] C. M. Crudden, M. Sateesh, R. Lewis, and C. Kl, “Mercaptopropyl-Modified Mesoporous Silica : A Remarkable Support for the Preparation of a Reusable , Heterogeneous Palladium Catalyst for Coupling Reactions synthesis , they suffer from one significant drawback , that they,” no. 16, pp. 10045–10050, 2005.
- [90] S. Chassaing, A. S. S. Sido, A. Alix, M. Kumarraja, P. Pale, and J. Sommer, “‘Click chemistry’ in zeolites: Copper(I) zeolites as new heterogeneous and ligand-free catalysts for the huisgen [3+2] cycloaddition,” *Chem. - A Eur. J.*, vol. 14, no. 22, pp. 6713–6721, 2008.
- [91] R. B. N. Baig and R. S. Varma, “Copper on chitosan: a recyclable

- heterogeneous catalyst for azide–alkyne cycloaddition reactions in water,” *Green Chem.*, vol. 15, no. 7, pp. 1839–1843, 2013.
- [92] T. Shamim and S. Paul, “Silica functionalized Cu(I) as a green and recyclable heterogeneous catalyst for the Huisgen 1,3-dipolar cycloaddition in water at room temperature,” *Catal. Letters*, vol. 136, no. 3–4, pp. 260–265, 2010.
- [93] R. Dey, B. Sreedhar, and B. C. Ranu, “Molecular sieves-supported palladium(II) catalyst: Suzuki coupling of chloroarenes and an easy access to useful intermediates for the synthesis of irbesartan, losartan and boscalid,” *Tetrahedron*, vol. 66, no. 13, pp. 2301–2305, 2010.
- [94] C. Cattivola, J. M. Fraile, J. I. García, and J. A. Mayoral, “A new titanium-silica catalyst for the epoxidation of alkenes,” *J. Mol. Catal. A Chem.*, vol. 112, no. 2, pp. 259–267, 1996.
- [95] L. Gu, D. Ma, S. Yao, C. Wang, W. Shen, and X. Bao, “Structured zeolites catalysts with hierarchical channel structure,” *Chem. Commun. (Camb.)*, vol. 46, no. 10, pp. 1733–5, 2010.
- [96] R. B. N. Baig and R. S. Varma, “A highly active and magnetically retrievable nanoferrite–DOPA–copper catalyst for the coupling of thiophenols with aryl halides,” *Chem. Commun.*, vol. 48, no. 20, p. 2582, 2012.
- [97] A. Schätz, M. Hager, and O. Reiser, “Cu(II)-Azabis(oxazoline)-Complexes Immobilized on superparamagnetic magnetite@silica-nanoparticles: A highly selective and recyclable catalyst for the kinetic resolution of 1,2-Diols,” *Adv. Funct. Mater.*, vol. 19, no. 13, pp. 2109–2115, 2009.

- [98] A. Schätz, R. N. Grass, Q. Kainz, W. J. Stark, and O. Reiser, “Cu(II)-Azabis(oxazoline) complexes immobilized on magnetic Co/C nanoparticles: Kinetic resolution of 1,2-Diphenylethane-1,2-diol under batch and continuous-flow conditions,” *Chem. Mater.*, vol. 22, no. 2, pp. 305–310, 2010.
- [99] R. N. Dhital *et al.*, “Low-temperature carbon-chlorine bond activation by bimetallic gold/palladium alloy nanoclusters: An application to Ullmann coupling,” *J. Am. Chem. Soc.*, vol. 134, no. 50, pp. 20250–20253, 2012.
- [100] K. H. Bleicher, H.-J. Böhm, K. Müller, and A. I. Alanine, “Hit and lead generation: beyond high-throughput screening,” *Nat. Rev. Drug Discov.*, vol. 2, no. 5, pp. 369–378, 2003.
- [101] J. F. Pritchard, M. Jurima-Romet, M. L. J. Reimer, E. Mortimer, B. Rolfe, and M. N. Cayen, “Making better drugs: Decision gates in non-clinical drug development.,” *Nat. Rev. Drug Discov.*, vol. 2, no. 7, pp. 542–553, 2003.
- [102] A. Padwa and W. H. Pearson, *Synthetic Applications of 1,3-Dipolar Cycloaddition Chemistry Toward Heterocycles and Natural Products*, vol. 59. 2002.
- [103] H. C. Kolb and K. B. Sharpless, “The growing impact of click chemistry on drug discovery,” *Drug Discov. Today*, vol. 8, no. 24, pp. 1128–1137, 2003.
- [104] H. C. Kolb, M. G. Finn, and K. B. Sharpless, “Click Chemistry: Diverse Chemical Function from a Few Good Reactions,” *Angewandte Chemie - International Edition*, vol. 40, no. 11. pp. 2004–2021, 2001.
- [105] I. S. Park, M. S. Kwon, Y. Kim, J. S. Lee, and J. Park, “Heterogeneous copper

- catalyst for the cycloaddition of azides and alkynes without additives under ambient conditions,” *Org. Lett.*, vol. 10, no. 3, pp. 497–500, 2008.
- [106] V. V. Rostovtsev, L. G. Green, V. V. Fokin, and K. B. Sharpless, “A stepwise Huisgen cycloaddition process: Copper(I)-catalyzed regioselective ‘ligation’ of azides and terminal alkynes,” *Angew. Chemie - Int. Ed.*, vol. 41, no. 14, pp. 2596–2599, 2002.
- [107] C. W. Tornøe, C. Christensen, and M. Meldal, “Peptidotriazoles on solid phase: [1,2,3]-Triazoles by regiospecific copper(I)-catalyzed 1,3-dipolar cycloadditions of terminal alkynes to azides,” *J. Org. Chem.*, vol. 67, no. 9, pp. 3057–3064, 2002.
- [108] A. Zarei, L. Khazdooz, A. R. Hajipour, H. Aghaei, and G. Azizi, “Microwave-assisted click chemistry synthesis of 1,2,3-triazoles from aryldiazonium silica sulfates in water,” *Synth.*, vol. 44, no. 21, pp. 3353–3360, 2012.
- [109] K. D. Bodine, D. Y. Gin, and M. S. Gin, “Synthesis of readily modifiable cyclodextrin analogues via cyclodimerization of an alkynyl-azido trisaccharide,” *J. Am. Chem. Soc.*, vol. 126, no. 6, pp. 1638–1639, 2004.
- [110] B. C. Suh, H. Jeon, G. H. Posner, and S. M. Silverman, “Vitamin D side chain triazole analogs via cycloaddition ‘click’ chemistry,” *Tetrahedron Lett.*, vol. 45, no. 24, pp. 4623–4625, 2004.
- [111] E.-H. Ryu and Y. Zhao, “Efficient synthesis of water-soluble calixarenes using click chemistry,” *Org. Lett.*, vol. 7, no. 6, pp. 1035–1037, 2005.
- [112] S. Löber, P. Rodriguez-Loaiza, and P. Gmeiner, “Click linker: Efficient and

- high-yielding synthesis of a new family of SPOS resins by 1,3-dipolar cycloaddition,” *Org. Lett.*, vol. 5, no. 10, pp. 1753–1755, 2003.
- [113] R. Manetsch *et al.*, “In Situ Click Chemistry: Enzyme Inhibitors Made to Their Own Specifications,” *J. Am. Chem. Soc.*, vol. 126, no. 40, pp. 12809–12818, 2004.
- [114] S. Cavalli, A. R. Tipton, M. Overhand, and A. Kros, “The chemical modification of liposome surfaces via a copper-mediated [3 + 2] azide-alkyne cycloaddition monitored by a colorimetric assay,” *Chem. Commun.*, no. 30, pp. 3193–3195, 2006.
- [115] J. L. Brennan *et al.*, “Bionanoconjugation via click chemistry: The creation of functional hybrids of lipases and gold nanoparticles,” *Bioconjug. Chem.*, vol. 17, no. 6, pp. 1373–1375, 2006.
- [116] D. Arosio, M. Bertoli, L. Manzoni, and C. Scolastico, “Click chemistry to functionalise peptidomimetics,” *Tetrahedron Lett.*, vol. 47, no. 22, pp. 3697–3700, 2006.
- [117] P. Wu *et al.*, “Efficiency and fidelity in a click-chemistry route to triazole dendrimers by the copper(I)-catalyzed ligation of azides and alkynes,” *Angew. Chemie - Int. Ed.*, vol. 43, no. 30, pp. 3928–3932, 2004.
- [118] B. Helms, J. L. Mynar, C. J. Hawker, and J. M. J. Fréchet, “Dendronized linear polymers via ‘click chemistry,’” *J. Am. Chem. Soc.*, vol. 126, no. 46, pp. 15020–15021, 2004.
- [119] R. Alvarez *et al.*, “HIV 1,2,3-triazoles,” *J. Med. Chem.*, vol. 37, pp. 4185–

4194, 1994.

- [120] S. Velázquez *et al.*, “Regiospecific synthesis and anti-human immunodeficiency virus activity of novel 5-substituted N-alkylcarbamoyl and N,N-dialkylcarbamoyl 1,2,3-triazole-TSAO analogues,” *Antivir. Chem. Chemother.*, vol. 9, no. 6, pp. 481–9, 1998.
- [121] M. J. Genin *et al.*, “Substituent effects on the antibacterial activity of nitrogen-carbon-linked (azolyphenyl)oxazolidinones with expanded activity against the fastidious gram-negative organisms *Haemophilus influenzae* and *Moraxella catarrhalis*,” *J. Med. Chem.*, vol. 43, no. 5, pp. 953–970, 2000.
- [122] D. R. Buckle and C. J. M. Rockell, “Studies on v-triazoles. Part 4. The 4-methoxybenzyl group, a versatile N-protecting group for the synthesis of N-unsubstituted v-triazoles,” *J. Chem. Soc. Perkin Trans. 1*, vol. 1982, p. 627, 1982.
- [123] Y. L. Angell and K. Burgess, “Peptidomimetics via copper-catalyzed azide–alkyne cycloadditions,” *Chem. Soc. Rev.*, vol. 36, no. 10, p. 1674, 2007.
- [124] V. D. Bock, H. Hiemstra, and J. H. Van Maarseveen, “Cu I-catalyzed alkyne–azide ‘click’ cycloadditions from a mechanistic and synthetic perspective,” *European J. Org. Chem.*, no. 1, pp. 51–68, 2006.
- [125] W. S. Horne, C. D. Stout, and M. R. Ghadiri, “A heterocyclic peptide nanotube,” *J. Am. Chem. Soc.*, vol. 125, no. 31, pp. 9372–9376, 2003.
- [126] M. A. Quraishi and D. Jamal, “Fatty Acid Triazoles: Novel Corrosion Inhibitors for Oil Well Steel (N-80) and Mild Steel,” *J. Am. oil Chem. Soc.*,

vol. 77, no. 10, pp. 1107–1111, 2000.

- [127] P. Douglas, J. D. Thomas, H. Strohm, C. Winscom, D. Clarke, and M. S. Garley, “Triplet energies and the singlet oxygen quenching mechanism for 7H-pyrazolo[5,1-c]-1,2,4-triazole azomethine dyes,” *Photochem. Photobiol. Sci.*, vol. 2, no. 5, pp. 563–568, 2003.
- [128] M. J. Paterson, M. A. Robb, L. Blancafort, and A. D. DeBellis, “Theoretical Study of Benzotriazole UV Photostability: Ultrafast Deactivation through Coupled Proton and Electron Transfer Triggered by a Charge-Transfer State,” *J. Am. Chem. Soc.*, vol. 126, no. 9, pp. 2912–2922, 2004.
- [129] Y. M. A. Yamada, S. M. Sarkar, and Y. Uozumi, “Amphiphilic self-assembled polymeric copper catalyst to parts per million levels: Click chemistry,” *J. Am. Chem. Soc.*, vol. 134, no. 22, pp. 9285–9290, 2012.
- [130] F. Himo *et al.*, “Copper(I)-catalyzed synthesis of azoles. DFT study predicts unprecedented reactivity and intermediates,” *J. Am. Chem. Soc.*, vol. 127, no. 1, pp. 210–216, 2005.
- [131] M. Malkoch *et al.*, “Structurally diverse dendritic libraries: A highly efficient functionalization approach using click chemistry,” *Macromolecules*, vol. 38, no. 9, pp. 3663–3678, 2005.
- [132] C. Ornelas, J. Ruiz Aranzaes, E. Cloutet, S. Alves, and D. Astruc, “Click Assembly of 1,2,3-Triazole-Linked Dendrimers, Including Ferrocenyl Dendrimers, Which Sense Both Oxo Anions and Metal Cations,” *Angew. Chemie*, vol. 119, no. 6, pp. 890–895, 2007.

- [133] A. K. Diallo, C. Ornelas, L. Salmon, J. R. Aranzaes, and D. Astruc, “‘Homeopathic’ catalytic activity and atom-leaching mechanism in Miyaura-Suzuki reactions under ambient conditions with precise dendrimer-stabilized Pd nanoparticles,” *Angew. Chemie - Int. Ed.*, vol. 46, no. 45, pp. 8644–8648, 2007.
- [134] T. Miao and L. Wang, “Regioselective synthesis of 1,2,3-triazoles by use of a silica-supported copper(I) catalyst,” *Synthesis (Stuttg.)*, no. 3, pp. 0363–0368, 2008.
- [135] C. Girard, E. Önen, M. Aufort, S. Beauvière, E. Samson, and J. Herscovici, “Reusable polymer-supported catalyst for the [3+2] Huisgen cycloaddition in automation protocols,” *Org. Lett.*, vol. 8, no. 8, pp. 1689–1692, 2006.
- [136] K. D. Karlin, R. W. Cruse, Y. Gultneh, A. Farooq, J. C. Hayes, and J. Zubieta, “Dioxygen-copper reactivity. Reversible binding of O₂ and CO to a phenoxo-bridged dicopper(I) complex,” *J. Am. Chem. Soc.*, vol. 109, no. 9, pp. 2668–2679, 1987.
- [137] A. Coelho, P. Diz, O. Caamaño, and E. Sotelo, “Polymer-supported 1,5,7-triazabicyclo [4.4.0] dec-5-ene as polyvalent ligands in the copper-catalyzed Huisgen 1,3-dipolar cycloaddition,” *Adv. Synth. Catal.*, vol. 352, no. 7, pp. 1179–1192, 2010.
- [138] T. Muraoka, C. Y. Koh, H. Cui, and S. I. Stupp, “Light-triggered bioactivity in three dimensions,” *Angew. Chemie - Int. Ed.*, vol. 48, no. 32, pp. 5946–5949, 2009.

- [139] T. Otsuka, T. Maeda, and A. Hotta, "Effects of salt concentrations of the aqueous peptide-amphiphile solutions on the sol-gel transitions, the gelation speed, and the gel characteristics," *J. Phys. Chem. B*, vol. 118, no. 39, pp. 11537–11545, 2014.
- [140] Z. Luo and S. Zhang, "Designer nanomaterials using chiral self-assembling peptide systems and their emerging benefit for society," *Chem. Soc. Rev.*, vol. 41, no. 13, p. 4736, 2012.
- [141] X. Zhao *et al.*, "Molecular self-assembly and applications of designer peptide amphiphiles.," *Chem. Soc. Rev.*, vol. 39, no. 9, pp. 3480–3498, 2010.
- [142] R. J. Mart, R. D. Osborne, M. M. Stevens, and R. V Ulijn, "Peptide-based stimuli-responsive biomaterials," *Soft Matter*, vol. 2, no. 10, pp. 822–835, 2006.
- [143] J. a Fallas, L. E. R. O'Leary, and J. D. Hartgerink, "Peptide and protein based materials in 2010: from design and structure to function and application," *Chem. Soc. Rev.*, vol. 39, no. 9, pp. 3510–27, 2010.
- [144] C. Veerman, K. Rajagopal, C. S. Palla, D. J. Pochan, J. P. Schneider, and E. M. Furst, "Gelation kinetics of β -hairpin peptide hydrogel networks," *Macromolecules*, vol. 39, no. 19, pp. 6608–6614, 2006.
- [145] A. Ghosh, M. Haverick, K. Stump, X. Yang, M. F. Tweedle, and J. E. Goldberger, "Fine-tuning the pH trigger of self-assembly," *J. Am. Chem. Soc.*, vol. 134, no. 8, pp. 3647–3650, 2012.
- [146] J. Y. Kim, M. H. Park, M. K. Joo, S. Y. Lee, and B. Jeong, "End groups

- adjusting the molecular nano-assembly pattern and thermal gelation of polypeptide block copolymer aqueous solution,” *Macromolecules*, vol. 42, no. 8, pp. 3147–3151, 2009.
- [147] Y. Wang, Y. Wang, G. Wu, Y. Fan, and J. Ma, “pH-Responsive Self-Assembly and conformational transition of partially propyl-esterified poly(L-aspartic acid) as amphiphilic biodegradable polyanion,” *Colloids Surfaces B Biointerfaces*, vol. 68, no. 1, pp. 13–19, 2009.
- [148] X. D. Xu, Y. Jin, Y. Liu, X. Z. Zhang, and R. X. Zhuo, “Self-assembly behavior of peptide amphiphiles (PAs) with different length of hydrophobic alkyl tails,” *Colloids Surfaces B Biointerfaces*, vol. 81, no. 1, pp. 329–335, 2010.
- [149] H. Xu *et al.*, “Hydrophobic-region-induced transitions in self-assembled peptide nanostructures,” *Langmuir*, vol. 25, no. 7, pp. 4115–4123, 2009.
- [150] L. Chen *et al.*, “Salt-induced hydrogelation of functionalised-dipeptides at high pH,” *Chem. Commun. (Camb)*, vol. 47, no. 44, pp. 12071–3, 2011.
- [151] V. Castelletto, I. W. Hamley, C. Cenker, and U. Olsson, “Influence of Salt on the Self-Assembly of Two Model Amyloid Heptapeptides,” *J. Phys. Chem. B*, vol. 114, no. 23, pp. 8002–8008, 2010.
- [152] M. M. Javadpour and M. D. Barkley, “Self-assembly of designed antimicrobial peptides in solution and micelles,” *Biochemistry*, vol. 36, no. 31, pp. 9540–9549, 1997.
- [153] H. Dong, S. E. Paramonov, L. Aulisa, E. L. Bakota, and J. D. Hartgerink,

- “Self-assembly of multidomain peptides: Balancing molecular frustration controls conformation and nanostructure,” *J. Am. Chem. Soc.*, vol. 129, no. 41, pp. 12468–12472, 2007.
- [154] J. Hentschel, E. Krause, and H. G. Börner, “Switch-peptides to trigger the peptide guided assembly of poly(ethylene oxide)-peptide conjugates into tape structures,” *J. Am. Chem. Soc.*, vol. 128, no. 24, pp. 7722–7723, 2006.
- [155] D. W. P. M. Löwik, J. Garcia-Hartjes, J. T. Meijer, and J. C. M. Van Hest, “Tuning secondary structure and self-assembly of amphiphilic peptides,” *Langmuir*, vol. 21, no. 2, pp. 524–526, 2005.
- [156] R. Polsky, J. C. Harper, D. R. Wheeler, S. M. Dirk, D. C. Arango, and S. M. Brozik, “Electrically addressable diazonium-functionalized antibodies for multianalyte electrochemical sensor applications,” *Biosens. Bioelectron.*, vol. 23, no. 6, pp. 757–764, 2008.
- [157] N. P. Westcott and M. N. Yousaf, “Synergistic microfluidic and electrochemical strategy to activate and pattern surfaces selectively with ligands and cells,” *Langmuir*, vol. 24, no. 6, pp. 2261–2265, 2008.
- [158] T. Okano, N. Yamada, M. Okuhara, H. Sakai, and Y. Sakurai, “Mechanism of cell detachment from temperature-modulated, hydrophilic-hydrophobic polymer surfaces1,” in *The Biomaterials: Silver Jubilee Compendium*, 2006, pp. 109–115.
- [159] A. L. Black, J. M. Lenhardt, and S. L. Craig, “From molecular mechanochemistry to stress-responsive materials,” *J. Mater. Chem.*, vol. 21,

- no. 6, pp. 1655–1663, 2011.
- [160] K. Nakayama, T. Tachikawa, and T. Majima, “Protein recording material: Photorecord/erasable protein array using a UV-eliminative linker,” *Langmuir*, vol. 24, no. 5, pp. 1625–1628, 2008.
- [161] I. Luzinov, S. Minko, and V. V. Tsukruk, “Responsive brush layers: from tailored gradients to reversibly assembled nanoparticles,” *Soft Matter*, vol. 4, no. 2007, p. 714, 2008.
- [162] C. Brieke, F. Rohrbach, A. Gottschalk, G. Mayer, and A. Heckel, “Light-controlled tools,” *Angewandte Chemie - International Edition*, vol. 51, no. 34, pp. 8446–8476, 2012.
- [163] A. A. Deeg, T. E. Schrader, S. Kempter, J. Pfizer, L. Moroder, and W. Zinth, “Light-triggered aggregation and disassembly of amyloid-like structures,” *ChemPhysChem*, vol. 12, no. 3, pp. 559–562, 2011.
- [164] K. Jarowicki and P. Kocienski, “Protecting groups,” *J. Chem. Soc. Perkin Trans. 1*, no. 16, pp. 2495–2527, 2000.
- [165] P. Klán *et al.*, “Photoremovable protecting groups in chemistry and biology: Reaction mechanisms and efficacy,” *Chem. Rev.*, vol. 113, no. 1, pp. 119–191, 2013.
- [166] V. N. Rajasekharan Pillai, “Photoremovable Protecting Groups in Organic Synthesis,” *Synthesis*, vol. 1980, no. 1, pp. 1–26, 1980.
- [167] M. Goeldner and R. S. Givens, *Dynamic Studies in Biology: Phototriggers*,

Photoswitches and Caged Biomolecules. 2005.

- [168] J. Cui, V. S. Miguel, and A. Del Campo, "Light-triggered multifunctionality at surfaces mediated by photolabile protecting groups," *Macromol. Rapid Commun.*, vol. 34, no. 4, pp. 310–329, 2013.
- [169] C. J. Bosques and B. Imperiali, "Photolytic control of peptide self-assembly," *J. Am. Chem. Soc.*, vol. 125, no. 25, pp. 7530–7531, 2003.
- [170] J. Cui, R. A. Gropeanu, D. R. Stevens, J. Rettig, and A. Del Campo, "New photolabile BAPTA-based Ca²⁺ cages with improved photorelease," *J. Am. Chem. Soc.*, vol. 134, no. 18, pp. 7733–7740, 2012.
- [171] G. C. Ellis-Davies, J. H. Kaplan, and R. J. Barsotti, "Laser photolysis of caged calcium: rates of calcium release by nitrophenyl-EGTA and DM-nitrophen.," *Biophys. J.*, vol. 70, no. 2, pp. 1006–16, 1996.
- [172] H. Hennings, D. Michael, C. Cheng, P. Steinert, K. Holbrook, and S. H. Yuspa, "Calcium regulation of growth and differentiation of mouse epidermal cells in culture.," *Cell*, vol. 19, no. 1, pp. 245–254, 1980.
- [173] C. L. Tu, Y. Oda, L. Komuves, and D. D. Bikle, "The role of the calcium-sensing receptor in epidermal differentiation," *Cell Calcium*, vol. 35, no. 3, pp. 265–273, 2004.
- [174] A. G. Szent-Györgyi, "Calcium regulation of muscle contraction.," *Biophys. J.*, vol. 15, no. 7, pp. 707–23, 1975.
- [175] A. Meir *et al.*, "Ion channels in presynaptic nerve terminals and control of

transmitter release,” *Physiol. Rev.*, vol. 79, no. 3, pp. 1019–1088, 1999.

- [176] J. Cui, M. Wang, Y. Zheng, G. M. Rodríguez Muñiz, and A. Del Campo, “Light-triggered cross-linking of alginates with caged Ca^{2+} ,” *Biomacromolecules*, vol. 14, no. 5, pp. 1251–1256, 2013.